Journal of Medicinal Chemistry



Article

# A Fragment Linking Approach Using 19F NMR Spectroscopy to Obtain Highly Potent and Selective Inhibitors of #-secretase.

John Brad Jordan, Douglas A. Whittington, Michael D. Bartberger, E. Allen Sickmier, Kui Chen, Yuan Cheng, and Ted Judd

*J. Med. Chem.*, **Just Accepted Manuscript** • DOI: 10.1021/acs.jmedchem.5b01917 • Publication Date (Web): 15 Mar 2016



## Just Accepted



ACS Publications

Journal of Medicinal Chemistry is published by the American Chemical Society. 1155 Sixteenth Street N.W., Washington, DC 20036

# A Fragment-Linking Approach Using $^{19}$F NMR Spectroscopy to Obtain Highly Potent and Selective Inhibitors of β-Secretase

*John B. Jordan*, Douglas A. Whittington, Michael D. Bartberger, E. Allen Sickmier, Kui Chen, Yuan Cheng and Ted Judd*

Therapeutic Discovery, Amgen, Inc. One Amgen Center Drive, Thousand Oaks, CA 91320

**RECEIVED DATE**

* To whom correspondence should be addressed. Tel: 805-313-5647. Fax: 805-480-1337. E-mail:brad.jordan@amgen.com

## Abstract

Fragment-based drug discovery (FBDD) has become a widely used tool in small molecule drug discovery efforts. One of the most commonly used biophysical methods in detecting weak binding of fragments is nuclear magnetic resonance (NMR) spectroscopy. In particular, FBDD performed with $^{19}$F NMR-based methods has been shown to provide several advantages over $^{1}$H NMR using traditional magnetization-transfer and/or two-dimensional methods. Here, we demonstrate the utility and power of $^{19}$F-based fragment screening by detailing the identification of a second-site fragment through $^{19}$F NMR screening that binds to a specific pocket of the aspartic acid protease, β-secretase (BACE-1). The identification of this second-site fragment allowed the undertaking of a fragment-linking approach, which ultimately yielded a molecule exhibiting a more than 360-fold increase in potency while maintaining reasonable ligand efficiency and gaining much improved selectivity over cathepsin-D (CatD). X-ray crystallographic studies of the molecules demonstrated that the linked fragments exhibited binding modes consistent with those predicted from the targeted screening approach, through-space NMR data, and molecular modeling.

## Introduction

Fragment-based drug discovery (FBDD) has rapidly gained momentum in the discovery and development of small molecule therapeutics. Over the past ten years, FBDD has become a common workstream in the path to find novel chemical matter, often for challenging targets, and a number of molecules in various phases of development have been derived from an initial fragment screening hit [1]. With the advent of FBDD came the necessity for highly sensitive biophysical methods aimed at detecting the weak binding of small molecules normally observed in fragment-based approaches. As such, various solution-phase NMR techniques and adaptations to surface plasmon resonance (SPR) methods (as well as other methods) have been utilized, both of which now comprise the majority of the biophysical toolbox used in high-throughput fragment screening.

The use of NMR in screening for fragment binding has historically utilized two main approaches: protein-detected and ligand-detected experiments. In protein-detected experiments, pioneered by Fesik and coworkers, the target of interest is typically labeled with the NMR-active $^{15}$N nucleus, and two-dimensional heteronuclear single-quantum coherence (HSQC) experiments are used to monitor the protein signals for changes upon ligand binding [2]. Conversely, typical ligand-detected approaches use unlabeled protein at low concentrations and rely on magnetization transfer pathways from either the protein itself (saturation transfer difference, or STD) or from bulk water (Water-Ligand Observe via Gradient SpectroscopY, or Water-LOGSY) to observe binding of the small molecule to the target of interest [3, 4]. More recently, we and others have discussed the use of $^{19}$F NMR spectroscopy in FBDD as a powerful tool in detecting weak binding of small molecules, and even as a potentially general strategy for fragment

screening by NMR [5]. The utility of using the fluorine nucleus as a highly sensitive detection method of weak binding is not a new development [4, 5, 6, 7]. However, here the use of $^{19}$F-based fragment screening is extended to so called "second-site" approaches, in which a known ligand is used to block one region of a target's pocket while another region is probed for small molecule binding using $^{19}$F NMR. In this example, this approach is applied to β-secretase, a potentially high-value target implicated in the onset and progression of Alzheimer's disease (AD).

BACE-1 is an aspartic protease that functions in the cleavage process of amyloid precursor protein (APP), an amyloidogenic pathway that ultimately yields shorter fragments of the Aβ peptide, including the pathogenic species Aβ40 and Aβ42, which are believed to play a primary role in the etiology of AD[8, 9, 10, 11]. The identification of potent ligands for BACE-1 has been met with some success by fragment-based approaches[12, 13, 14]. A number of papers have detailed results of fragment screening against BACE-1 by various methods, and many of those fragments have been optimized through structure-based design to yield potent, and even *in vivo* efficacious, inhibitors of BACE-1[12, 13, 14, 15, 16]. In addition, recent publications have detailed extensive structure activity relationship (SAR) efforts to obtain suitable selectivity of BACE-1 inhibitors against cathepsin D (CatD), a related aspartic protease residing in lysosomes[17]. It has been observed that the acidic environment of lysosomes results in the accumulation of traditionally charged BACE-1 inhibitors[17], resulting in much higher local concentrations of the molecules and thereby presenting problems with off-target inhibition of other lysosomal enzymes, such as CatD. Off-target inhibition of CatD is of great potential concern, having been proposed to be involved in ocular as well as neurodegenerative side-effects[18]. For this reason, a very high degree of selectivity against CatD and other lysosomal enzymes is necessary, and thus, CatD

inhibition is a commonly used selectivity filter for small molecule inhibitors of BACE-1 [17, 19]. There are some distinct structural differences in the binding pockets between BACE-1 and CatD, the most prominent being the nature and composition of the S3 pocket in BACE-1. Utilization of the S3 pocket by appropriate chemical matter has been shown to enhance CatD selectivity[17]. We postulated that further extension of a lead molecule past the S3 pocket and down into the $S3_{subpocket}$ would afford additional selectivity. Thus, one of our primary aims in this work was to use FBDD to find a second-site ligand to the $S3_{subpocket}$ of BACE-1 that could subsequently be linked to the core compound that would afford both an increase in potency and, importantly, a higher degree of CatD selectivity.

One of the founding principles of FBDD, as originally described using SAR by NMR [2], is that leads can be rapidly derived from weakly binding fragments due to the fact that the binding energies of multiples fragments can be additive.[20, 21, 22] Thus, linking a second-site ligand with an affinity of ~ 1mM with a first-site ligand could theoretically yield a potency gain of three orders of magnitude.[22] This, of course, is neglecting any effects on affinity due to entropic factors or from the linker design itself. The fragment-linking approach has been well documented over the last decade and has proven to be a viable approach to small molecule drug discovery[20, 21, 22, 23]. However, these approaches are not trivial, and many times several iterations of linkers are required to provide optimal conformations of the ligand. It is often more common to find that the observed fragment linking additivity is less than the theoretical additivity than it is to find that they meet or exceed the theoretical gains in affinity [2, 23].

In attempts to apply fragment-based methods to the design of potent and selective small molecule inhibitors of BACE-1, a molecule derived from a core fragment and resulting from early-stage SAR was used to serve as blocking compound for a large portion of the BACE-1 pocket, thereby allowing a "second-site" fragment screen to be conducted. Using this method of fragment linking, $^{19}$F-NMR based fragment screening has been applied to identify chemical matter that binds specifically to the S3 and $S3_{subpocket}$ of BACE-1. Upon identification of fragments binding the "blocked" conformation of BACE-1, inter-ligand NOE NMR experiments and molecular modeling led to the chemical linkage of the two compounds (core + fragment) and yielded compounds with both increased on-target potency (~350x) as well as improved selectivity (~2000x) against CatD.

## Results and Discussion

The use of $^{19}$F NMR in screening campaigns, particularly in fragment-based approaches, has been previously detailed [4, 6, 7]. In FBDD, the use of $^{19}$F NMR has many benefits; the major one being the utilization of the fluorine nucleus for a very sensitive detection tool for weak binding. Other attributes of using $^{19}$F as a detection tool have been reviewed extensively by Dalvit and others[4, 7]. In the realm of sensitivity, the $^{19}$F nucleus is almost as sensitive as that of a proton (with a gyromagnetic ratio about 0.83 that of $^{1}$H), and the lack of a protonated background in $^{19}$F-NMR enables the use of solvents, buffers, or detergents that would normally interfere with a typical $^{1}$H-based NMR screening campaign; thereby increasing the effective sensitivity. This high sensitivity allows the detection of small quantities of compounds (~20 μM) in very short experiment times (3–4 min). Also, The $^{19}$F nucleus is characterized by a large chemical shift dispersion (~200 ppm) and very narrow line widths ($\Delta_{w1/2}$ ~ 1–2 Hz) that allow screening to be

conducted on large pools of compounds without the concern of signal overlap[5]. Standard $^{1}$H-based NMR fragment screening experiments such as STD or LOGSY are performed in pools of five compounds or less [24]. $^{19}$F-NMR, however, allows the screen to be conducted on pools of compounds containing up to 20 compounds-all possessing unique chemical shifts. This effectively negates the need for any specific pooling strategy when designing libraries.

In approaching the second-site fragment screen for BACE-1, a suitable blocking molecule was needed to facilitate the identification of a true S3 pocket binder. Previously, Cheng et al. presented data demonstrating the elaboration of a 2-aminoquinoline fragment ($K_D$ ~ 900 μM) to a molecule with an affinity of 11 pM [13]. In a semi-parallel effort to the traditional structure-based design efforts in this study, a second-site fragment screen was attempted using our in-house $^{19}$F fragment library in an attempt to find additional chemical matter that would allow the linking of a core molecule to a fragment that was targeted to occupy the S3 binding site of BACE-1. Compound 58 from Cheng et al. (compound **1** in Table 1) was used in the fragment screens as a blocking compound to occupy the majority of the binding site of BACE-1 ($K_D$ ~ 16 nM) while leaving the S3 and $S3_{subpocket}$ regions accessible (Figure 1A). Next, the $^{19}$F-NMR fragment screen was performed with saturating concentrations (~ 5 μM) of compound **1** in the experimental buffer.The NMR signals of the $^{19}$F nucleus are extremely sensitive to changes in the environment surrounding the fluorine[5]. When the free and protein-bound fractions of the fluorine containing compound experience significantly different environments, broadening of the NMR signals occurs with a concomitant decrease in signal intensity. In all, the screen yielded seven fragments that exhibited binding to the target in the presence of the blocking compound. As depicted in Figure 2, the fluorine NMR signals of the ligands that bind to BACE-1 can

experience significant linebroadening, resulting in an obvious decrease in signal intensity upon binding to the larger protein. Following the screen, the binder with highest affinity (as determined by the effect on the NMR lineshape and by SPR) was used in a competition binding assay to determine if the fragment indeed bound to the desired pocket. To do this, a more potent inhibitor (Compound **2**, $K_D$ ~ 600 pM, Table 1) from the aminooxazoline xanthene series [17] that occupied all of the binding pockets in question (Figure 1B) was used as a competitor with the blocking compound **1** and the newly identified fragment (compound **3**). As evidenced in Figure 2, the fragment alone failed to bind the protein, but clearly did so in the presence of the blocking compound. Upon the addition of the competitor compound (compound **2**), the $^{19}$F NMR signal from the fragment became sharp again, suggesting that the competitor molecule replaced a substantial fraction of the fragment in the binding site, resulting in a higher concentration of free compound (fragment) in solution and a sharpening of the NMR signal. In addition, the fragment failed to exhibit binding to CatD both in the presence and absence of the blocking compound (Figure 2). These data were highly suggestive that the $^{19}$F fragment was indeed binding to the S3 and/or $S3_{subpocket.}$ It should be noted that the displacement of the fragment was not complete in the competition assay; this was likely due to the poor solubility of the competitor molecule. However, in all cases tested, addition of the more potent inhibitor that fully occupied the S3 site resulted in significant sharpening of the $^{19}$F signals, indicating the increased presence of unbound ligand.

In order to determine the affinity of each fragment to BACE-1, surface plasmon resonance (SPR) experiments were used in the presence of saturating concentrations of the blocking compound (compound **1**, 5 μM). Three molecules exhibited binding to the blocked form of BACE-1 with

affinities in the 100-300 μM range, with four more compounds exhibiting much weaker binding (Supplementary Figure 1). In particular, compound **3** stood out in its affinity to BACE-1 in the presence of the blocking compound. Furthermore, this compound exhibited undetectable binding to BACE-1 in the absence of the blocking compound (Figure 3, in agreement with the NMR data (Figure 2), and suggesting that the presence of the blocking compound helped to define the binding pocket for the fragment.

Taken together, these results were highly suggestive that compound **3** was indeed binding specifically to the S3 and $S3_{subpocket}$ of BACE-1. Based on the theory of fragment additivity, two fragments can be linked together to ultimately form a more potent compound. The extent of potency increases, however, is dictated by factors such as linker design, rigid body entropy, and even synergistic binding. A simplistic view to approximate the benefits of linking two fragment is the simple multiplicative effect of the two affinities ($K_A$*$K_B$) [20, 21, 23].However, it affinities commonly fail to reach the optimal potency due to imperfect linker design or other entropic effects. Due to the high relative affinity of compound **3** compared to the other fragments (Figure S1), this molecule was selected as the lead fragment, and further experiments were conducted to determine if a fragment-linking strategy was viable.

With the knowledge that compound **3** likely bound specifically to the S3 site, a strategy was designed that would allow the linkage of compound **3** to a core molecule enabling direct access to the S3 and $S3_{subpocket}$ regions. From historical structural data, it was known that replacement of the pyridine ring of compound **1** with a toluyl ring at the 6-position of the core aminoquinoline allowed the ortho-methyl group to flip, and face directly toward the S3 pocket (compound **5**, and

structure in Fig 1C). This particular trajectory provided a direct line into the S3 pocket with which the linked molecule could possibly gain additional potency and selectivity against CatD. In order to test this hypothesis inter-ligand NOE (ILNOE) NMR experiments [25] were used in an attempt to identify the proximity and orientation of the bound fragment relative to another compound of known binding mode (Figure 4). For these experiments, a weaker 2-aminoquinoline tool molecule with a toluyl substitution at the 6 position of 2-aminoquinoline (compound **4**) was used as a probe ($K_D$ ~ 20 μM) to allow for strong NOEs between the methyl group and any protons of the $^{19}F$ fragment. As shown in Figure 4, NOEs were clearly observed between the ortho- methyl group of the tool compound (**4**) and the 1, 2, and 3 protons of the chloropyridine moiety of the fragment (**3**). These data, along with structural data from compound **5** suggested that the ortho-methyl group of the tool compound and chloropyridine moiety of the fragment were within 5-6 Å from each other and that the fluorophenyl group of the $^{19}F$ fragment likely extended down into the hydrophobic $S3_{subpocket}$ of BACE-1. These results served to guide modeling efforts in attempts to design adequate linkers of these two compounds.

Using the spatial and orientation data obtained from the ILNOE experiments, molecular modeling studies were used to propose potential linking approaches to attach compound **3** onto the already potent core 2-aminoquinoline (compound **5**). With the observed orientation of the toluyl substituent (providing a nearly direct trajectory into the S3 region) coupled with the likely binding orientation of a benzamide S3 moiety (i.e. engagement of the Gly230 carbonyl by the amide NH and occupancy of the $S3_{subpocket}$ by the para-substituted arene) various rigidified linking agents were computationally probed via docking of the lowest energy adduct conformers into the BACE-1 active site. In all, four hybrid molecules, possessing linkers which were

predicted to dispose the resultant pendent benzamide substituent in a manner described above, were proposed for synthesis (Figure 5)

Upon completion of the syntheses of compounds **6-9**, the compounds were tested for binding to BACE-1 by SPR. All of the compounds exhibited a reasonable improvement in affinity (Figure 6, Table 2). However, conjugation of the fragment to the core molecule did result in a modest decrease in ligand efficiency (LE) (Table 2) with compound **9** staying close to the generally targeted LE of 0.3. To test for potency and selectivity both *in vitro and in vivo,* the compounds were tested in BACE-1 enzyme and cellular assays along with a CatD enzyme assay. (Table 2 and Figure S2). All compounds exhibited reasonable improvements in $IC_{50}$ values compared to the parent compound both *in vitro* and *in vivo*. However, compound **9** exhibited a roughly 350-fold gain in its affinity for BACE and only a 16-fold cell shift (compared with a cell shift of 380 for the parent molecule).[13] Most importantly, however, this particular compound exhibited ~2000-fold increase in selectivity against CatD (in both enzyme and cell assays) with respect to the parent compound (see data in Table 2 and Figure S2).

To thoroughly investigate the binding mode of the linked molecules, the compounds were submitted for X-ray crystallography in order to determine if the fluorophenyl group of the $^{19}F$ fragment was indeed binding in the S3 site. High quality X-ray structures were determined for two of the compounds thereby demonstrating unequivocally that the binding mode of the final compounds was consistent with the experimental results. In the crystal structure of BACE-1 with compound **6** (Figure 7a), the aminoquinoline portion of the inhibitor engages the catalytic aspartic acid residues as expected and the flexible aliphatic chain extending off from the

aminoquinoline bends around and occupies the S1' and S2' pockets and forms a hydrogen bond with Gly34, as observed in the crystal structure of compound **5**. As predicted, the alkynyl linkage is oriented such that the cyclopropyl moiety binds in the S1 pocket and the fluorophenyl ring occupies the S3 pocket and part of the $S3_{subpocket}$. In this position, compound **6** forms a hydrogen bond between its amide NH and the backbone carbonyl oxygen atom of Gly230 and between its amide carbonyl oxygen atom and a water molecule that in turn interacts with the backbone of Phe108. In the crystal structure of BACE-1 with compound **9** (Figure 7B), many similar features are observed including interactions with the protein made by the aminoquinoline portion of the inhibitor derived from the original blocking compound. In place of the alkyne linker of compound **6**, however, compound **9** contains two methylene groups that allow a nearly 90° torsion angle to be made, enabling the pyridine ring to sit on the surface of the protein in the S1 pocket. The edge of the pyridine ring also makes van der Waals interactions with the face of the aminoquinoline ring. The amide NH of the inhibitor forms a hydrogen bond to Gly230 and while the amide moiety largely fills the S3 pocket, the fluorophenyl ring pushes deeply into the $S3_{subpocket}$. These extensive interactions between compound **9** and BACE-1 likely account for its excellent *in vitro* and *in vivo* potency, and the deeper penetration of the fluorophenyl ring of compound **9** into the $S3_{subpocket}$, relative to compound **6**, likely results in its higher selectivity over CatD. The crystallographic results also demonstrate why certain compounds, such as compound **3**, have stronger binding interactions in the presence of the blocking compound than in its absence.

## Conclusion

We have demonstrated here the utility of $^{19}$F-NMR in a fragment-based approach to designing potent and selective small molecule inhibitors of BACE-1 using a fragment linking approach. The final compound presented here was derived from a 2-aminoquinoline fragment originally proposed by Astex [14] and structure-based drug design was used to optimize this compound into a highly potent molecule[13]. Here, we demonstrate that $^{19}$F-NMR based fragment approaches are a rapid means to identify additional chemical matter that can be used in fragment-linking approaches to allow a higher degree of molecular diversity.

## Materials and Methods

**NMR Spectroscopy.** All NMR experiments were performed on a Bruker Avance III NMR spectrometers (Bruker Biospin, Billerica, MA) operating at a $^{1}$H frequency of 500.13 MHz or 800.12 MHz. $^{19}$F experiments were conducted using a SEF cryogenic probe equipped for direct $^{19}$F detection while proton experiments were acquired at 800 MHz on a TCI cryoprobe. One dimensional $^{19}$F spectra were acquired for each sample at 283 K using $^{1}$H decoupling with a spectra width of 71428 Hz, an acquisition time of 917 ms, and 128 scans with a relaxation delay of 1 s. This yielded experiment times on the order of 6 min each, and allowing 2 min for initial temperature equilibration. This experimental set up allowed all reference and screen spectra to be acquired in less than 24 h. The $^{19}$F fragment screen for BACE-1 was conducted in 50 mM Sodium Acetate, pH 5.0, 100 mM NaCl, and 5% D2O (for field frequency lock). Protein and compound concentrations for the fragment screen were 10 μM and 20 μM, respectively.

Two-dimensional Inter-ligand NOE (ILNOE) experiments [25] were conducted in a similar buffer (except using deuterated components) using a standard two-dimensional $^{1}H$-$^{1}H$ NOESY pulse sequence on an 800 MHz Bruker Avance III NMR spectrometer using a 500 ms mixing time and spectral widths of 8169 Hz (in F1 and F2) and 2048 and 512 data points in the direct and indirect dimensions, respectively.

All data were processed using Topspin 3.2 (Bruker Biospin, Billerica, MA) and were then compared visually to the reference spectra using the spectral overlay feature. Hits were identified by signal intensity and/or chemical shift changes. Since each compound in a pool had a unique chemical shift, hit identification was straightforward, and hit compounds could be identified by simply matching the chemical shift of the hit compound to that found in the compound database.

**Surface Plasmon Resonance Spectroscopy**

Dissociation constant ($K_D$) measurements were performed on Biacore S51 and SensiQ Pioneer FE SPR instruments (GE Healthcare and SensiQ Technologies, respectively). BACE-1 protein and inhibitors for SPR measurements were generated in-house; all other reagents were purchased from GE Healthcare, SensiQ or Sigma-Aldrich. Glycosylated BACE-1 was reacted with sodium periodate to oxidize *cis*-diol groups on sugar chains to aldehydes. The oxidized BACE-1 was immobilized at high density (10000–12000 RU) onto either a CM5 or COOH5 sensor chip (GE Healthcare and SensiQ Technologies, respectively) using aldehyde coupling chemistry and resulted in surface activities close to 100% based on reference inhibitor binding. The immobilization running buffer consisted of 10 mM HEPES pH 7.4 with 150 mM NaCl and immobilization steps consisted of a 3–4 min EDC/NHS activation step [200 mM 1-ethyl-3-(3-

dimethylaminopropyl) carbodiimide hydrochloride, 50 mM *N*-hydroxysuccinimide], 7 min 5 mM carbohydrizide in water, 7 min 1 M ethanolamine hydrochloride pH 8.5, 10 min 20 μg/mL oxidized BACE-1 in 10 mM sodium acetate pH 4.0, 7 min 100 mM sodium cyanoborohydride in 100 mM sodium acetate pH 4.0, 3 × 30 s 50 mM glycine pH 9.5 and 3 × 30 s 1 M NaCl in 100 mM $NaHCO_3$ pH 9.5. The reference spot for all SPR experiments consisted of the blank surface of the sensor chip treated in an identical manner as the other flow cell spot excluding the addition of protein.

For $K_D$ measurements, the buffer was replaced with 50 mM sodium acetate pH 5.0, 150 mM NaCl, 0.005 (v/v) Tween-20, and 2% (v/v) DMSO. Compound stocks prepared in DMSO (typically 20 mM) were serially diluted in running buffer and injected over the immobilized BACE-1. Association and dissociation time were typically set to 45 s and 90 s, respectively. However, in the case of the more potent compounds, dissociation times were extended in some cased to 20 minutes. All SPR experiments were performed at 25 °C with a flow rate of 30 μL/min and data collection rate of 10 Hz.

The data were processed and analyzed using either Scrubber-2 analysis software (BioLogic Software, Campbell, Australia) or QDat (SensiQ Technologies, Oklahoma City, OK). The sample response observed on the reference spot was subtracted from the sample response with immobilized BACE-1 to correct for systematic noise and baseline drift. Data was solvent corrected and the response from blank injections was used to double-reference the binding data. The data were molecular weight normalized and $K_D$ values established using either simple steady analysis or single-site kinetic fit using a mass transport term ($k_m$).

**Molecular Modeling.**

Low-energy conformers for a variety of potential adducts possessing various rigidifying elements (alkynyl, cyclopropyl, etc. linkages) were generated with the MMFF94 force field as implemented in the MOE program suite[26] while constraining the aminoquinoline warhead and S1'-S2' atoms to their positions found in the crystal structure of **1** (Figure 1). The resultant conformers were then subjected to MM-GBSA minimization in the BACE-1 active site (rigid protein model) using the AMBER94 / GAFF force field as implemented in AMBER 9.0[27] Adducts possessing the best predicted binding affinities and which best presented the pendent benzamide NH in an orientation favorable for hydrogen bonding to the Gly230 carbonyl oxygen were proposed for synthesis.

**X-ray Crystallography.** The catalytic domain of human BACE-1 was expressed as inclusion bodies, purified, and apo crystals were grown as described previously [28]. The co-crystal structures of BACE-1 with compounds **1**,**2**, and **5** bound were obtained by soaking apo crystals in modified mother liquor solution (25 % PEG 5000 MME, 0.1 M sodium citrate, pH 6.6, 0.2 M ammonium iodide, 3% (v/v) dimethylsulfoxide) containing 0.5 mM compound for 6 hours at room temperature. The crystals were then transferred briefly to the same solution supplemented with 20% (v/v) glycerol prior to flash-cooling for data collection. In order to obtain co-crystal structures of BACE-1 with compounds **6** and **9**, concentrated protein at ~6 mg/mL was mixed with 0.5 mM inhibitor and incubated on ice for 90 min. The protein-inhibitor complexes were crystallized by hanging drop vapor diffusion at room temperature by mixing 1 µL of protein with 1 µL of precipitant solution (1.4-1.5 M ammonium sulfate, 0.2 M lithium chloride and either 0.1 M bis-tris (pH 5.5) or 0.1 M MES (pH 6.0)); wells contained 0.5 mL of precipitant solution.

Single crystals appeared within 1 - 2 weeks. Prior to data collection, crystals were transferred briefly into cryo solutions consisting of mother liquor supplemented with 20% (v/v) glycerol and flash-cooled in liquid nitrogen. Diffraction data for co-crystals with compounds **9** and **12** were collected at SER-CAT beam line 22-BM at the Advanced Photon Source using a MAR225 CCD detector and $\lambda$ = 1.0000 Å. Apo BACE-1 crystals soaked with compounds **1**, **2**, and **5** had data collected at the Advanced Light Source, beamline 5.0.2, using an ADSC Q315 CCD detector and $\lambda$ = 1.0000 Å. Images were processed with HKL2000 [29] and the structures were refined using REFMAC [30]. Model building was performed with COOT [31]. Data collection and refinement statistics appear in Table S1 of the Supporting Information.

**BACE-1 Enzymatic Assay**

BACE-1and CatD enzymatic activity was determined by the enhancement of fluorescence intensity upon enzymatic cleavage of the fluorescence resonance energy transfer substrate. The BACE-1 recognition and cleavage sequence of the substrate is derived from the reported literature[32], and the fluorophore and quencher dyes were attached to side chain of Lys residues at the termini of the substrate peptide. The human recombinant BACE-1[33]assay was performed in 50 mM acetate, pH 4.5, 8% DMSO, 100 μM Genepol, and 0.002% Brij-35. In dose–response $IC_{50}$ assays, 10 point 1:3 serial dilutions of compound in DMSO were pre-incubated with the enzyme for 60 min at room temperature. Subsequently, the substrate was added to initiate the reaction. After 60 min at room temperature, the reaction was stopped by addition of 0.1 M Tris base to raise the pH above the enzyme active range, and the increase of fluorescence intensity was measured on Safire II microplate reader (Tecan, Männedorf, Switzerland).

**Chemistry.** Unless otherwise noted, all materials were obtained from commercial suppliers and were used without further purification. All final compounds were purified to ≥95% purity as determined by high-performance liquid chromatography (HPLC).

**Synthesis of N-(1-(3-(2-bromophenyl) prop-2-yn-1-yl)cyclopropyl)-4-fluorobenzamide used in the synthesis of Compound 6.**

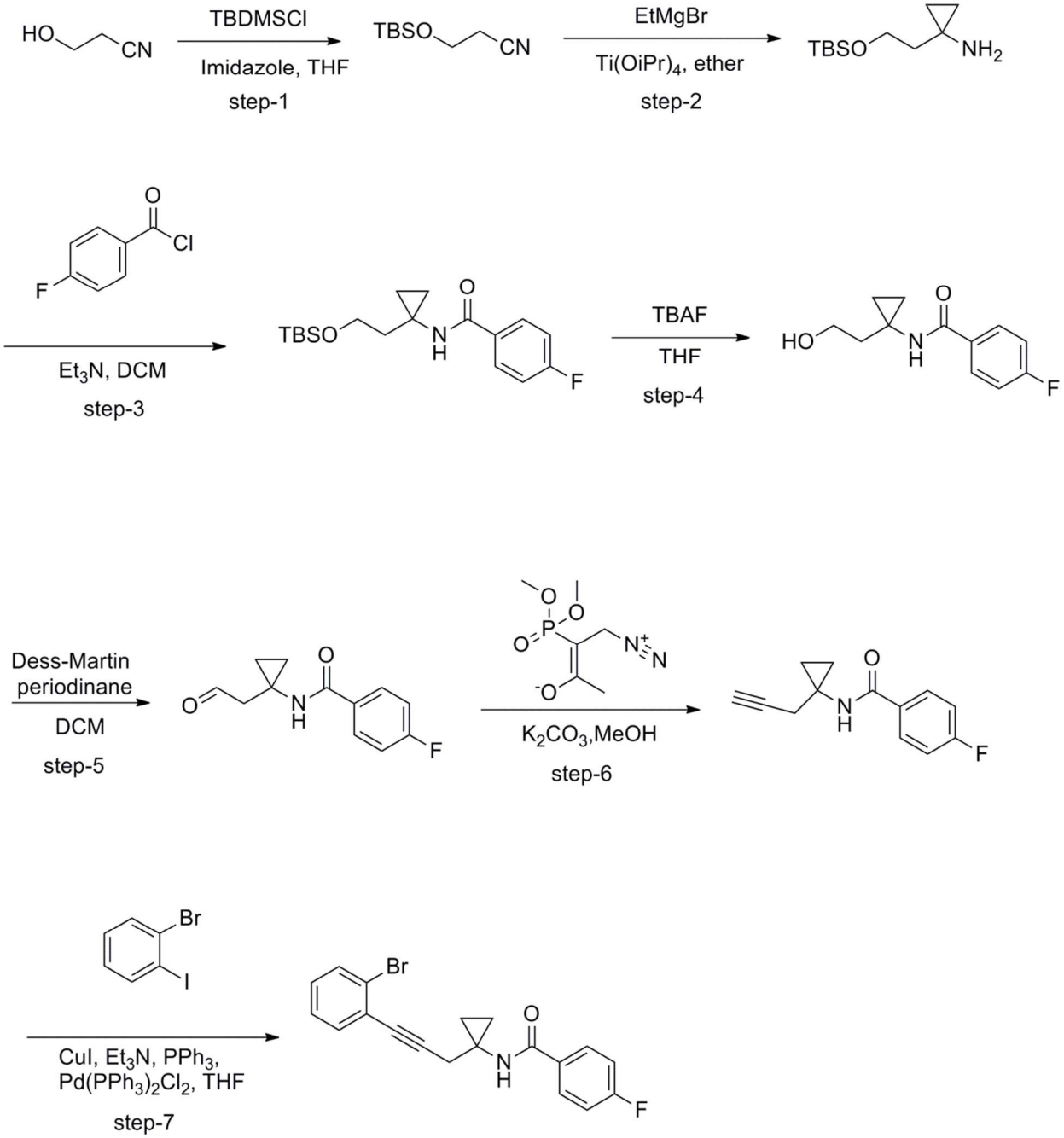

**Step 1: Synthesis of 3-((tert-butyldimethylsilyl) oxy) propanenitrile:** To a solution of 3-hydroxypropanenitrile (10 g, 141 mmol, 1 equiv) in tetrahydrofuran (200 mL) at 0 °C, was added imidazole (23.94 g, 352 mmol, 2.5 equiv) followed by tert-butyldimethylsilyl chloride (TBDMS-Cl) (25.4 g, 169 mmol, 1.2 equiv). After the addition was completed, the reaction mixture was stirred at room temperature for 16 h. After completion of the reaction (monitored by TLC), the mixture was quenched with water (20 mL) and extracted with ethyl acetate (2 x 100 mL). The combined organic layers were washed with brine (50 mL), dried over $Na_2SO_4$ and concentrated in vacuo to give the crude material as light-yellow oil. The crude material was purified by flash column chromatography (silica gel, 230-400 mesh), eluting with a gradient of 0 to 10% ethyl acetate in hexane to provide 3-((tert-butyldimethylsilyl) oxy) propanenitrile (20 g, 108 mmol, 77 % yield) as a colorless liquid. $^1$H NMR (400 MHz, Chloroform-*d*) δ 3.86 (t, *J* = 6.4 Hz, 2H), 2.56 (t, *J* = 6.3 Hz, 2H), 0.93 (s, 9H), 0.11 (s, 6H).

**Step 2: Synthesis of 1-(2-((tert-butyldimethylsilyl)oxy)ethyl)cyclopropan-1-amine:** To a solution of 3-((tert-butyldimethylsilyl) oxy) propanenitrile (20 g, 108 mmol, 1.0 equiv) in diethyl ether (200 mL), was added titanium (IV) isopropoxide (53.8 mL, 183 mmol, 1.7 equiv) at 0 °C. Ethylmagnesium bromide (90 mL, 270 mmol, 2.5 equiv, 3.0 M in diethyl ether) was added slowly. After addition, the reaction mixture was stirred at room temperature for 1 h and again cooled to 0 °C. To this mixture, boron trifluoride etherate was added (54.7 mL, 216 mmol, 2.0 equiv, 50 % solution) dropwise. After addition, the reaction mixture was stirred at room temperature for 1 h. After completion of the reaction (monitored by TLC), the mixture was quenched with 10% sodium hydroxide solution (150 mL) and extracted with ethyl acetate (2 x 150 mL). The combined organic layer was washed with brine (50 mL), dried over $Na_2SO_4$ and

concentrated in vacuo to give the crude material as brown liquid. The crude material was purified by flash chromatography column (silica gel, 230-400 mesh), eluting with a gradient of 0 to 10% Ethyl acetate in hexane to provide 1-(2-((tert-butyldimethylsilyl)oxy)ethyl)cyclopropan-1-amine (10 g, 46.4 mmol, 43 % yield) as a brown liquid. $^1$H NMR (300 MHz, Chloroform-*d*) δ 3.89 (d, *J* = 5.9 Hz, 2H), 2.92 (s, 2H), 1.69 (d, *J* = 5.9 Hz, 2H), 0.91 (s, 9H), 0.77 – 0.74 (m, 2H), 0.54 – 0.51 (m, 2H), 0.12 (s, 6H).

**Step 3: Synthesis of N-(1-(2-((tert-butyldimethylsilyl) oxy) ethyl) cyclopropyl)-4-fluorobenzamide:** To a solution of 1-(2-((tert-butyldimethylsilyl)oxy)ethyl)cyclopropan-1-amine (10 g, 46.4 mmol, 1.0 equiv) and triethylamine (9.71 mL, 69.6 mmol, 1.5 equiv) in dichloromethane (100 mL) cooled to 0 °C, was added 4-fluorobenzoyl chloride(8.83 g, 55.7 mmol, 1.2 equiv). After addition, the reaction mixture was stirred at room temperature for 3 h. After completion of the reaction (monitored by TLC), the mixture was quenched with water (100 mL) and extracted with dichloromethane (2 x 50 mL). The combined organic layer was washed with brine (50 mL), dried over $Na_2SO_4$ and concentrated in vacuo to give the crude material (light-yellow oil). The crude material was purified by flash column chromatography (silica gel, 230-400 mesh), eluting with a gradient of 0 to 10% ethyl acetate in hexane, to provide N-(1-(2-((tert-butyldimethylsilyl) oxy) ethyl) cyclopropyl)-4-fluorobenzamide (6 g, 17.78 mmol, 38.3 % yield) as light yellow solid. MS (ESI positive ion) m/z: 338.2 (M+1). $^1$H NMR (300 MHz, Chloroform-*d*) δ 7.76 – 7.72 (m, 2H), 7.12 – 7.07 (m, 2H), 6.54 (s, 1H), 3.82 (t, *J* = 5.9 Hz, 2H), 1.90 (t, *J* = 6.1 Hz, 2H), 0.96 – 0.94 (m, 2H), 0.87 (s, 9H), 0.84 – 0.80 (m, 2H), 0.04 (s, 6H).

**Step 4: Synthesis of 4-fluoro-N-(1-(2-hydroxyethyl)cyclopropyl)benzamide:** To a solution of N-(1-(2-((tert-butyldimethylsilyl) oxy) ethyl) cyclopropyl)-4-fluorobenzamide (6 g, 17.78 mmol,

1.0 equiv ) in tetrahydrofuran (60 mL) was added tetra-N-butylammonium fluoride (35.6 mL, 35.56 mmol, 2.0 equiv, 1.0 M in tetrahydrofuran) at room temperature and stirred at room temperature for 3 h. After completion of the reaction (monitored by TLC), the reaction mixture was quenched with water (60 mL) and extracted with ethylacetate (2 x 60 mL). The organic layer was washed with brine (30 mL) and dried over $Na_2SO_4$. The solution was filtered and concentrated in vacuo to give the crude material (light-yellow solid), which was purified by flash column chromatography (silica gel, 230-400 mesh), eluting with a gradient of 0 to 30% Ethyl acetate in hexane to provide 4-fluoro-N-(1-(2-hydroxyethyl)cyclopropyl)benzamide (2.8 g, 12.54 mmol, 70.6 % yield) as an off white solid. MS (ESI positive ion) m/z: 224.2 (M+1). $^1$H NMR (400 MHz, Chloroform-*d*) δ 7.79 – 7.75 (m, 2H), 7.15 – 7.10 (m, 2H), 6.54 (s, 1H), 3.76 – 3.73 (m, 2H), 1.79 – 1.76 (m, 2H), 1.00 – 0.90 (m, 4H).

**Step 5: Synthesis of 4-fluoro-N-(1-(2-oxoethyl)cyclopropyl)benzamide:** To a solution of 4-fluoro-N-(1-(2-hydroxyethyl)cyclopropyl)benzamide (1.0 g, 4.48 mmol, 1.0 equiv) in dichloromethane (30 mL), was added Dess-Martin periodinane (2.85 g, 6.72 mmol, 1.5 equiv) at 0 °C and then stirred at room temperature for 3 h. After completion of the reaction (monitored by TLC), the reaction was quenched with 10 % sodium bicarbonate (50 mL) and extracted with dichloromethnae (2 x 50 mL). The organic layer was washed with brine (10 mL) and dried over $Na_2SO_4$. The solution was filtered and concentrated in vacuo to give the crude material (light-yellow gum) which was purified by flash column chromatography (silica gel, 230-400 mesh), eluting with a gradient of 0 to 20% ethyl acetate in hexane to provide 4-fluoro-N-(1-(2-oxoethyl)cyclopropyl)benzamide (0.5 g, 2.26 mmol, 50.5 % yield), as an off white solid.

MS (ESI positive ion) m/z: 222.2 (M+1). $^{1}$H NMR (400 MHz, Chloroform-*d*) δ 9.85 (s, 1H), 7.76 – 7.71 (m, 2H), 7.13 – 7.08 (m, 2H), 6.77 (s, 1H), 2.92 (s, 2H), 1.04 – 1.01 (m, 2H), 0.87 – 0.85 (m, 2H).

**Step 6: Synthesis of 4-fluoro-N-(1-(prop-2-yn-1-yl) cyclopropyl) benzamide:** To a solution of 4-fluoro-N-(1-(2-oxoethyl)cyclopropyl)benzamide (500 mg, 2.26 mmol, 1.0 equiv) and potassium carbonate (1.2 g, 9.04 mmol, 4.0 equiv) in methanol (10 mL), was added dimethyl (1-diazo-2-oxo-propyl) phosphonate (521 mg, 2.71 mmol, 1.2 equiv) at 0 °C. After addition, the reaction mixture was stirred at room temperature for 4 h. After completion of the reaction (monitored by TLC), the mixture was quenched with water (15 mL) and extracted with ethyl acetate (2 x 20 mL). The organic layer was washed with brine (5 mL) and dried over $Na_2SO_4$. The solution was filtered and concentrated in vacuo to give the crude material (light-yellow gum) which was purified by flash column chromatography (silica gel, 230-400 mesh), eluting with a gradient of 0 to 10% Ethyl acetate in hexane to provide 4-fluoro-N-(1-(prop-2-yn-1-yl) cyclopropyl) benzamide (300 mg, 1.38 mmol, 61.1 % yield), as a light yellow solid.
MS (ESI positive ion) m/z: 218.2 (M+1). $^{1}$H NMR (300 MHz, Chloroform-*d*) δ 7.78 – 7.74 (m, 2H), 7.14 – 7.08 (m, 2H), 6.55 (s, 1H), 2.70 (s, 2H), 2.00 (t, $J$ = 2.6 Hz, 1H), 0.99 – 0.94 (m, 4H).

**Step 7: Synthesis of N-(1-(3-(2-bromophenyl) prop-2-yn-1-yl)cyclopropyl)-4-fluorobenzamide:** To a solution of 4-fluoro-N-(1-(prop-2-yn-1-yl) cyclopropyl) benzamide (300 mg, 1.381 mmol, 1.0 equiv) in tetrahydrofuran (10 mL), was added 1-iodo-2-bromo-benzene (391 mg, 1.381 mmol, 1.0 equiv), triethylamine (210 mg, 2.071 mmol, 1.5 equiv), triphenyl

phosphine (18.11 mg, 0.069 mmol, 0.05 equiv) and copper(I) iodide (26.3 mg, 0.138 mmol, 0.1 equiv) at room temperature. The reaction mixture was degassed with nitrogen, bis(triphenylphosphine)palladium(II)chloride (48.5 mg, 0.069 mmol, 0.05 equiv) was added, and the reaction mixture stirred at room temperature for 4 h. After completion (monitored by TLC), the reaction was quenched with water (15 mL), and extracted with ethyl acetate (2 x 10 mL). The organic layer was washed with brine (3 mL), and the organic extract was dried over $Na_2SO_4$. The solution was filtered and concentrated in vacuo to give the crude material. The crude product was purified by flash column chromatography (silica gel, 230-400 mesh), eluting with a gradient of 0 to 10% Ethyl acetate in hexane to provide N-(1-(3-(2-bromophenyl) prop-2-yn-1-yl)cyclopropyl)-4-fluorobenzamide (250 mg, 0.672 mmol, 48.6 % yield) as an off white solid. MS (ESI positive ion) m/z: 372.0 (M+). $^1$H NMR (300 MHz, Chloroform-*d*) δ 7.81 – 7.75 (m, 2H), 7.56 (d, *J* = 8.0 Hz, 1H), 7.43 – 7.40 (m, 1H), 7.24 – 7.07 (m, 4H), 6.70 (s, 1H), 2.95 (s, 2H), 1.06 – 0.96 (m, 4H).

**Synthesis of Compound 6.**

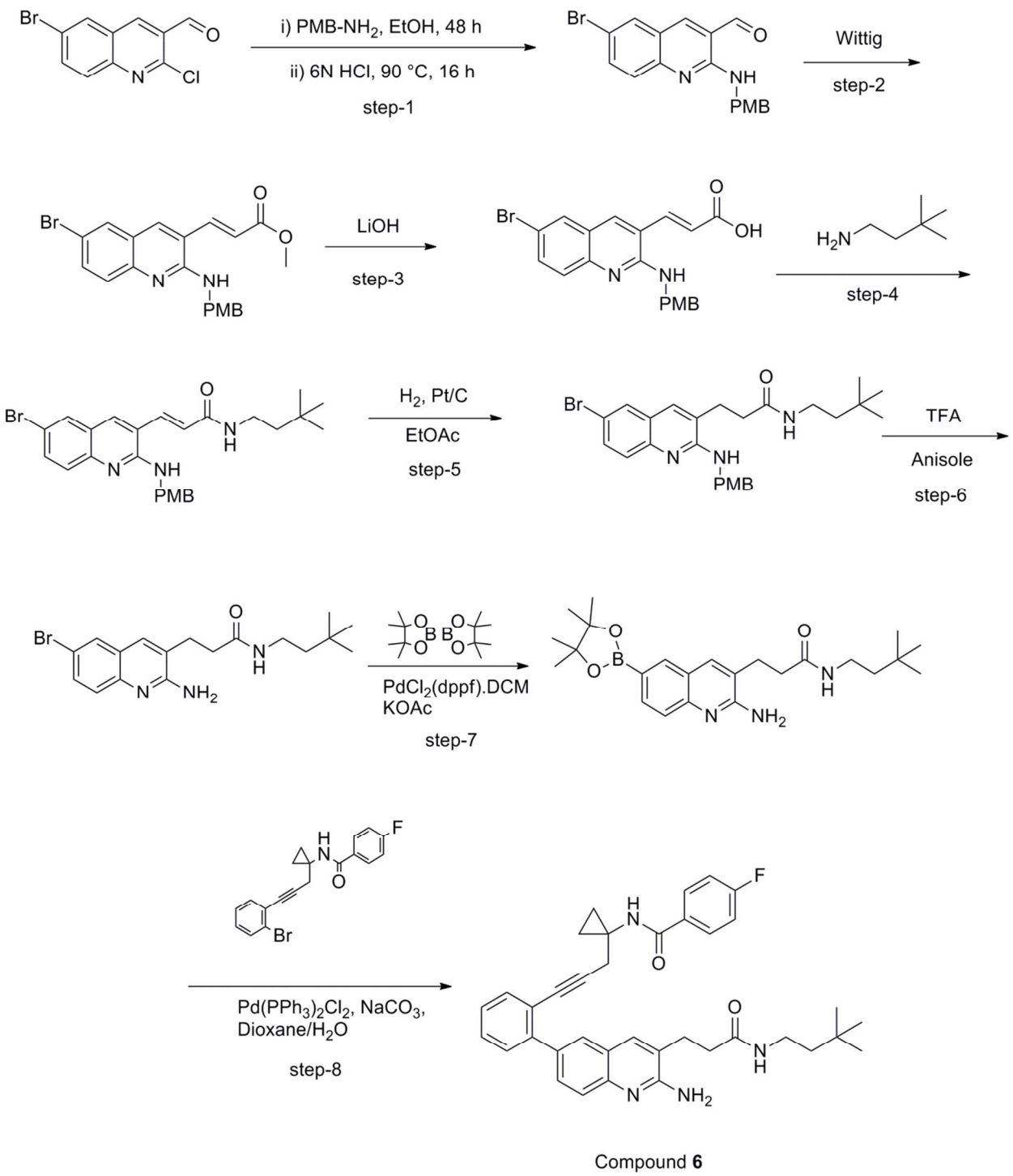


**Step 1: Synthesis of 6-bromo-2-((4-methoxybenzyl)amino)quinoline-3-carbaldehyde.** To a solution of 6-bromo-2-chloroquinoline-3-carbaldehyde (10 g, 37.0 mmol, 1.0 equiv) in absolute ethanol (200 mL in 1 L sealed tube) was added 4-methoxy benzyl amine (10.56 mL, 81 mmol,

2.2 equiv) at room temperature and the mixture was heated to 90 °C for 24 h. The reaction was not completed as indicated by thin layer chromatography (TLC). This reaction mixture was cooled to room temperature and added 4-methoxy benzyl amine (4.8 mL, 37 mmol, 1.0 equiv), then heated to 95 °C for additional 24 h. Once the reaction was completed (monitored by TLC), the reaction mixture was cooled to room temperature and aqueous 6N HCl was added (50 mL) and then heated to 90 °C for 24 h. After completion of the reaction (monitored by LC-MS), the reaction mixture was cooled to room temperature and ethanol was removed under vacuum. The resulting solid was washed with water (3 x 30 mL), methanol (2 x 5 mL) and dried to afford 6-bromo-2-((4-methoxybenzyl) amino) quinoline-3-carbaldehyde (**2**, 10 g, 72.9%) as a yellow solid. MS (ESI positive ion) m/z: 371.0, 373.0 (M+, M+2). $^{1}$H NMR (400 MHz, Chloroform-*d*) δ 10.05 (s, 1H), 8.49 (br s, 1H), 8.24 (s, 1H), 7.88 – 7.74 (m, 3H), 7.38 (d, *J* = 8.4 Hz, 2H), 6.90 (d, *J* = 8.4 Hz, 2H), 4.88 (s, 2H), 3.85 (s, 3H).

**Step 2: Synthesis of methyl 3-(6-bromo-2-((4-methoxybenzyl) amino) quinolin-3-yl) acrylate:** To a solution of 6-bromo-2-((4-methoxybenzyl)amino)quinoline-3-carbaldehyde (5 g, 13.47 mmol, 1.0 equiv) in anhydrous dicholormethane (100 mL) at 0 °C was added methyl 2-(triphenylphosphoranylidene)acetate (4.50 g, 13.47 mmol, 1.0 equiv) under a nitrogen atmosphere and the reaction was stirred at room temperature for 3 h. After completion of the reaction (monitored by TLC), the reaction mixture was concentrated under vacuum. The crude material was purified by flash column chromatography (silica gel, 230-400 mesh) using 15 to 20% of ethyl acetate in petroleum ether as an eluent to afford methyl 3-(6-bromo-2-((4-methoxybenzyl)amino)quinolin-3-yl)acrylate (3.76 g, 65.3%) as a yellow solid. MS (ESI positive ion) m/z: 427.0, 429.0 (M+, M+2). $^{1}$H NMR (300 MHz, Chloroform-*d*) δ 7.85 (s, 1H), 7.75 –

7.61 (m, 4H), 7.35 (d, *J* = 8.76 Hz, 2H), 6.93 – 6.87 (m, 2H), 6.47 (d, *J* = 15.7 Hz, 1H), 5.01 (br s, 1H), 4.74 (d, *J* = 5.1 Hz, 2H), 3.82 (s, 6H).

**Step 3: Synthesis of (E)-3-(6-bromo-2-((4-methoxybenzyl)amino)quinolin-3-yl)acrylic acid:** To a solution of compound methyl 3-(6-bromo-2-((4-methoxybenzyl) amino) quinolin-3-yl) acrylate (3.6 g, 8.43 mmol, 1.0 equiv) in tetrahydrofuran (40 mL) and water (40 mL) was added lithium hydroxide mono hydrate (0.404 g, 16.85 mmol, 2.0 equiv) at room temperature. After addition, the reaction mixture was stirred at room temperature for 4 h. After completion of the reaction (monitored by TLC), the reaction was quenched with water (40 mL) and extracted with ethyl acetate (2 x 60 mL). The combined organic extract was dried over $Na_2SO_4$ and concentrated in vacuo to provide (E)-3-(6-bromo-2-((4-methoxybenzyl)amino)quinolin-3-yl)acrylic acid (3.4 g, 8.23 mmol, 98 % yield) as a light yellow solid. MS (ESI positive ion) m/z: 413 (M+). $^1$H NMR (300 MHz, DMSO-$d_6$) δ 8.59 (s, 1H), 8.06 (s, 1H), 7.90 – 7.85 (m, 3H), 7.40 (d, *J* = 8.6 Hz, 2H), 6.91 (d, *J* = 8.6 Hz, 2H), 6.64 (d, *J* = 15.3 Hz, 1H), 4.85 (s, 2H), 3.72 (s, 3H).

**Step 4: Synthesis of (E)-3-(6-bromo-2-((4-methoxybenzyl)amino)quinolin-3-yl)-N-(3,3-dimethylbutyl)acrylamide:** To a solution of (E)-3-(6-bromo-2-((4-methoxybenzyl)amino)quinolin-3-yl)acrylic acid (3.4 g, 8.23 mmol, 1.0 equiv) in dichloromethane (100 mL), was added triethylamine (5.73 mL, 41.1 mmol, 5.0 equiv) and 2,4,6-tripropyl-1,3,5,2,4,6-trioxatriphosphinane 2,4,6-trioxide (7.85 g, 12.34 mmol, 1.5 equiv) in 50% Ethyl acetate/dichloromethane at room temperature. The mixture was then cooled to 0 °C and 3,3-dimethylbutan-1-amine (0.999 g, 9.87 mmol, 1.2 equiv) was added. After addition, the reaction mixture was warmed up to room temperature and stirred for 16 h. After completion

(monitored by TLC) of the reaction, the reaction was quenched with water (60 mL) and extracted with ethyl acetate (2 x 60 mL). The organic layer was washed with brine solution (30 mL), and the organic extract was dried over $Na_2SO_4$. The solution was filtered and concentrated in vacuo to give the crude material as a light yellow solid. The crude material was purified by flash column chromatography (silica gel, 230-400 mesh), eluting with a gradient of 0 to 30% Ethyl acetate in hexane, to provide (E)-3-(6-bromo-2-((4-methoxybenzyl)amino)quinolin-3-yl)-N-(3,3-dimethylbutyl)acrylamide (2.5 g, 5.04 mmol, 61.2 % yield), as a light yellow solid. MS (ESI positive ion) m/z: 496.0, 498.0 (M+, M+2). $^1$H NMR (400 MHz, Chloroform-*d*) δ 7.78 – 7.61 (m, 5H), 7.36 (d, *J* = 8.5 Hz, 2H), 6.89 (d, *J* = 8.5 Hz, 2H), 6.38 (d, *J* = 15.1 Hz, 1H), 5.60 (s, 1H), 5.10 (s, 1H), 4.74 (s, 2H), 3.84 (s, 3H), 3.44 – 3.38 (m, 2H), 1.52 – 1.48 (m, 2H), 0.98 (s, 9H).

**Step 5: Synthesis of 3-(6-bromo-2-((4-methoxybenzyl)amino)quinolin-3-yl)-N-(3,3-dimethylbutyl)propanamide:** To a solution of (E)-3-(6-bromo-2-((4-methoxybenzyl)amino)quinolin-3-yl)-N-(3,3-dimethylbutyl)acrylamide (1 g, 2.014 mmol, 1.0 equiv) in ethylacetate (20 mL), was added 10 % platinum on carbon (100 mg, 10 wt%) at room temperature. After addition, the reaction mixture was stirred under hydrogen pressure (5 psi) at room temperature for 4 h. After completion (monitored by LCMS), the reaction mixture was passed through a celite bed and washed with ethyl acetate (100 mL). The filtrate was concentrated in vacuo to yield 3-(6-bromo-2-((4-methoxybenzyl)amino)quinolin-3-yl)-N-(3,3-dimethylbutyl)propanamide (1 g, 2.006 mmol, 100 % yield) as a light yellow solid. MS (ESI positive ion) m/z: 498.0, 500.0 (M+, M+2). $^1$H NMR (400 MHz, Chloroform-*d*) δ 7.68 (d, *J* = 2.1 Hz, 1H), 7.63 – 7.56 (m, 2H), 7.50 (s, 1H), 7.39 (d, *J* = 8.5 Hz, 2H), 6.89 (d, *J* = 8.6 Hz, 2H),

5.69 (s, 1H), 5.32 (s, 1H), 4.75 (d, *J* = 5.1 Hz, 2H), 3.81 (s, 3H), 3.24 – 3.18 (m, 2H), 2.93 (t, *J* = 7.1 Hz, 2H), 2.49 (t, *J* = 7.1 Hz, 2H), 1.33 – 1.28 (m, 2H), 0.90 (s, 9H).

**Step 6: Synthesis of 3-(2-amino-6-bromoquinolin-3-yl)-N-(3,3-dimethylbutyl)propanamide:** To a solution of 3-(6-bromo-2-((4-methoxybenzyl)amino)quinolin-3-yl)-N-(3,3-dimethylbutyl)propanamide (500 mg, 1.003 mmol, 1.0 equiv) in trifluroacetic acid (10 mL), was added anisole (1096 µl, 10.03 mmol, 10 equiv) at room temperature. After addition, the reaction mixture was stirred at 50 °C for 3 h. After completion of the reaction (monitored by TLC), the reaction mixture was concentrated and then diluted with ethyl acetate (40 mL). The organic layer was washed with 10% $NaHCO_3$ solution (10 mL) and water (5 mL), dried over $Na_2SO_4$ and finally concentrated in vacuo to yield the crude 3-(2-amino-6-bromoquinolin-3-yl)-N-(3,3-dimethylbutyl)propanamide (300 mg, 0.793 mmol, 79 % yield) as a light yellow solid. MS (ESI positive ion) m/z: 378.0 (M+). $^1$H NMR (400 MHz, DMSO-$d_6$) δ 7.83 – 7.80 (m, 2H), 7.79 (s, 1H), 7.52 (d, *J* = 8.8 Hz, 1H), 7.37 (d, *J* = 8.8 Hz, 1H), 6.49 (s, 2H), 3.06 – 3.00 (m, 2H), 2.80 (t, *J* = 7.2 Hz, 2H), 2.43 (t, *J* = 7.2 Hz, 2H), 1.27 – 1.22 (m, 2H), 0.87 (s, 9H).

**Step 7: Synthesis of 3-(2-amino-6-(4,4,5,5-tetramethyl-1,3,2-dioxaborolan-2-yl)quinolin-3-yl)-N-(3,3-dimethylbutyl)propanamide:** To a solution of 3-(2-amino-6-bromoquinolin-3-yl)-N-(3,3-dimethylbutyl)propanamide (300 mg, 0.793 mmol, 1.0 equiv) in 1,4-dioxane (6 mL), was added potassium acetate (233 mg, 2.379 mmol, 3.0 equiv) and bis(pinacolato)diboron (242 mg, 0.952 mmol, 1.2 equiv). The mixture was then degassed with nitrogen, and $PdCl_2$(dppf)-$CH_2Cl_2$ (32.4 mg, 0.040 mmol, 0.05 equiv) was added at room temperature. After addition, the reaction mixture was stirred at 85 °C for 4 h. After completion of the reaction (monitored by TLC), the

mixture was quenched with water (6 mL) and extracted with ethyl acetate (2 x 15 mL). The organic extract was dried over $Na_2SO_4$ and concentrated in vacuo to give the crude material which was passed through a bed of silica gel (for removing of inorganics) to provide the crude 3-(2-amino-6-(4,4,5,5-tetramethyl-1,3,2-dioxaborolan-2-yl)quinolin-3-yl)-N-(3,3-dimethylbutyl)propanamide (400 mg) as a brown solid. MS (ESI positive ion) m/z: 426.2 (M+1).

**Step 8: Synthesis of N-(1-(3-(2-(2-amino-3-(3-((3,3-dimethylbutyl)amino)-3-oxopropyl)quinolin-6-yl)phenyl)prop-2-yn-1-yl)cyclopropyl)-4-fluorobenzamide (Compound 6):** To a solution of 3-(2-amino-6-(4,4,5,5-tetramethyl-1,3,2-dioxaborolan-2-yl)quinolin-3-yl)-N-(3,3-dimethylbutyl)propanamide (65 % purity, 175 mg, 0.267 mmol, 1.0 equiv) and N-(1-(3-(2-bromophenyl) prop-2-yn-1-yl)cyclopropyl)-4-fluorobenzamide (100 mg, 0.267 mmol, 1.0 equiv) taken in 1,4-dioxane (4 mL) and water (1 mL), was added sodium carbonate (56.7 mg, 0.535 mmol, 2.0 equiv). The mixture was then degassed with nitrogen. Bis(triphenylphosphine)palladium(II)chloride (9.38 mg, 0.013 mmol, 0.05 equiv) was added at room temperature and the reaction mixture stirred at 85 °C for 4 h. After completion of the reaction (monitored by TLC), the reaction mixture was quenched with water (5 mL) and extracted with ethyl acetate (2 x 20 mL). The organic extract was dried over $Na_2SO_4$ and concentrated in vacuo to give the crude material as a brown gum. The crude material was purified by flash column chromatography (silica gel, 230-400 mesh), eluting with a gradient of 0 to 30% methanol in chloroform, to provide 100 mg Compound **6**, which was further purified by preparative HPLC [YMC C8 (20 x 250mm, 5µ); mobile phase: 10 mM $NH_4OAc$ in water and acetonitrile; flow rate: 18 mL/min]. After concentration, the residue was mixed with water and extracted with dichloromethane. The organic extract was dried over $Na_2SO_4$ and evaporated

under reduced pressure. The residue was washed with hexane and lyophilized to provide Compound **6** (14 mg, 0.024 mmol, 8.86 % yield), as an off white solid. MS (ESI positive ion) m/z: 591.2 (M+1). $^{1}$H NMR (400 MHz, DMSO-$d_6$) δ 8.70 (s, 1H), 7.84 – 7.81 (m, 3H), 7.72 – 7.71 (m, 2H), 7.65 (dd, $J$ = 8.4, 2.0 Hz, 1H), 7.51 (d, $J$ = 7.6 Hz, 1H), 7.44 – 7.39 (m, 3H), 7.34 – 7.29 (m, 1H), 7.25 – 7.21 (m, 2H), 6.40 (s, 2H), 3.06 – 3.00 (m, 2H), 2.88 – 2.78 (m, 4H), 2.42 (t, $J$ = 7.6 Hz, 2H), 1.28 – 1.26 (m, 2H), 0.83 (s, 9H), 0.70 – 0.67 (m, 4H); $^{19}$F NMR (400 MHz, DMSO-$d_6$) δ -109.4.

**Synthesis of Compound 7.**

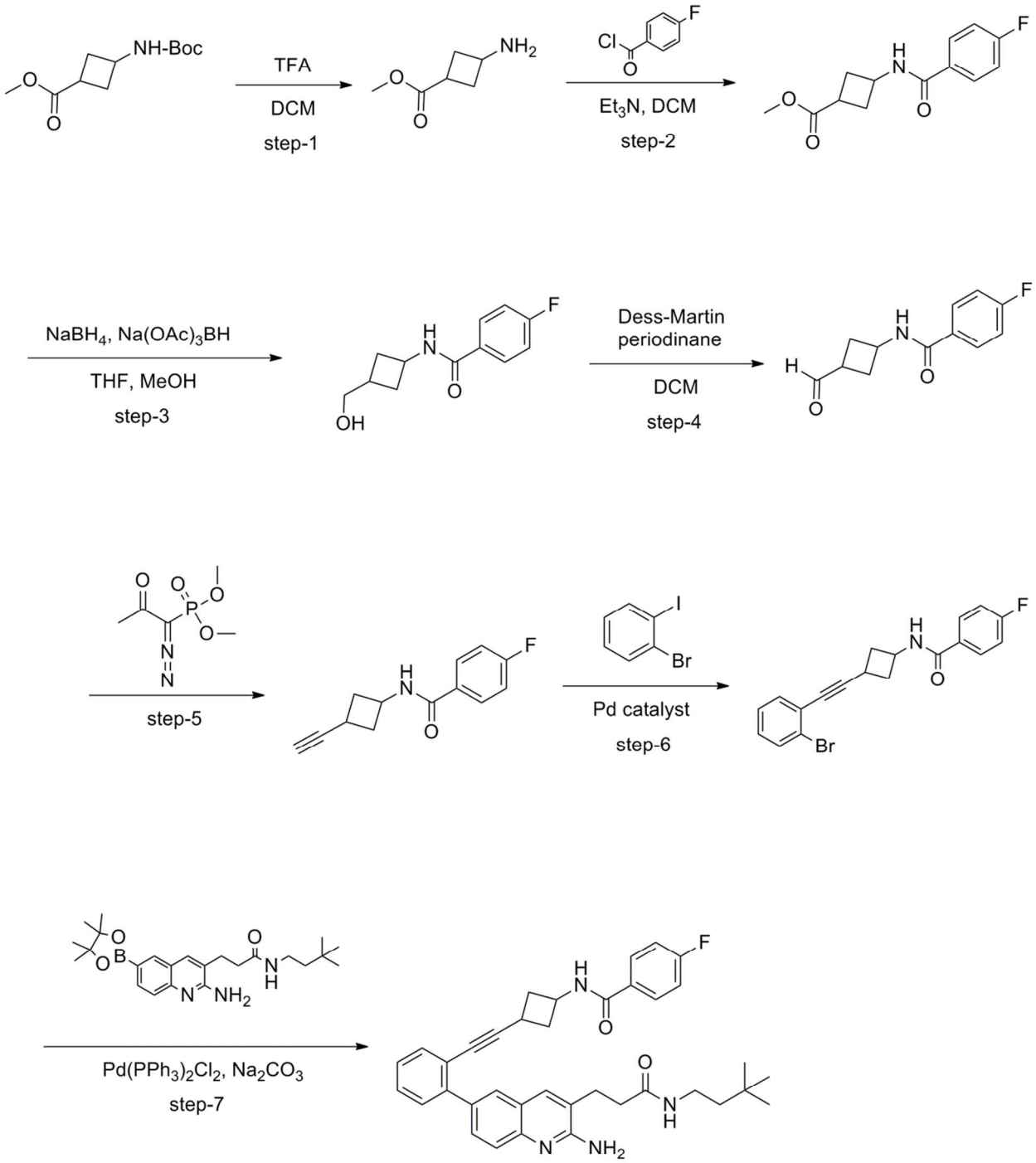


Compound **7**

**Step 1: Synthesis of methyl 3-aminocyclobutane-1-carboxylate:** To a solution of methyl 3-((tert-butoxycarbonyl)amino)cyclobutanecarboxylate (2 g, 8.72 mmol, 1.0 equiv) in dichloromethane (3 mL) at 0 °C was added dropwise trifluoroacetic acid (6.64 mL, 87 mmol, 10 equiv) under nitrogen atmosphere and stirred at room temperature for 2 h. After completion of the reaction (monitored by TLC), the excess TFA was removed by concentration under vacuum (kept bath temperature below 40 °C). To the resulting mixture was added methanol (5 mL) followed by solid sodium bicarbonate (5 g) and the reaction was stirred for 10 min. The reaction mixture was diluted with DCM (45 mL), filtered through celite pad and washed with dichloromethane:methanol (9:1, 3 x 20 mL). The filtrate was concentrated under vacuum to yield methyl 3-aminocyclobutanecarboxylate (1.05 g, 93%) as a colorless liquid. MS (ESI positive ion) m/z: 130.2 (M+1). $^{1}$H NMR (300 MHz, DMSO-$d_6$) δ 7.96 (s, 2H), 3.64 – 3.51 (m, 4H), 3.01 – 2.89 (m, 1H), 2.44 – 2.37 (m, 2H), 2.27 – 2.18 (m, 2H).

**Step 2: Synthesis of methyl 3-(4-fluorobenzamido)cyclobutane-1-carboxylate (3):** To the suspension of methyl 3-aminocyclobutanecarboxylate (1.0 g, 7.74 mmol, 1.0 equiv) in anhydrous DCM (10 mL) was added triethylamine (1.62 mL, 11.61 mmol, 1.5 equiv) at room temperature under nitrogen atmosphere and cooled to 0 °C. 4-Fluorobenzoyl chloride (1.0 mL, 8.52 mmol, 1.1 equiv) was added drop wise to the above reaction mixture and stirred at room temperature for 2 h. After completion of the reaction (monitored by TLC), the reaction mixture was quenched with ice-cold water (10 mL) and separated into biphasic layers. The aqueous layer was extracted with DCM (10 mL), and the combined organic layers were dried over anhydrous $Na_2SO_4$ and concentrated under vacuum. The crude material was purified by flash column chromatography

(silica gel, 230-400 mesh) using 25 to 30% of ethyl acetate in petroleum ether as an eluent to afford methyl 3-(4-fluorobenzamido)cyclobutanecarboxylate (1.9 g, 98%) as a white solid. MS (ESI positive ion) m/z: 252.0 (M+1).

$^1$H NMR (400 MHz, Chloroform-*d*) δ 7.82 – 7.78 (m, 2H), 7.13 (d, *J* = 8.6 Hz, 2H), 6.45 (d, *J* = 8.3 Hz, 1H), 4.68 – 4.58 (m, 1H), 3.75 (s, 3H), 2.98 – 2.89 (m, 1H), 2.80 – 2.73 (m, 2H), 2.28 – 2.20 (m, 2H).

**Step 3: Synthesis of 4-fluoro-N-(3-(hydroxymethyl)cyclobutyl)benzamide:** To a cooled solution of methyl 3-(4-fluorobenzamido)cyclobutanecarboxylate (1.45 g, 5.77 mmol, 1.0 equiv) in anhydrous THF (15 mL) and methanol (0.93 mL, 23.08 mmol, 4.0 equiv) at 0 °C was added sodium triacetoxyborohydride (0.122 g, 0.577 mmol, 0.1 equiv) followed by portion wise addition of sodium borohydride (0.284 g, 7.50 mmol, 1.3 equiv) under nitrogen atmosphere; the reaction was left stirring at room temperature for 16 h. After completion of the reaction (monitored by TLC), the reaction mixture was cooled to 0 °C and quenched with aqueous 10% $NaHCO_3$ solution (15 mL) and stirred for 15 min at room temperature. The reaction mixture was then extracted with ethyl acetate (3 x 15 mL) and combined organic layers were washed with brine (15 mL), dried over anhydrous $Na_2SO_4$ and concentrated under vacuum. The crude compound was purified by flash column chromatography (silica gel, 230-400 mesh) using 60 to 80% of ethyl acetate in petroleum ether as an eluent to afford 4-fluoro-N-(3-hydroxymethyl)cyclobutyl)benzamide (1.2 g, 93%) as a white solid. MS (ESI positive ion) m/z: 224.2 (M+1).$^1$H NMR (400 MHz, DMSO-$d_6$) δ 8.57 (d, *J* = 7.5 Hz, 1H), 7.94 – 7.89 (m, 2H), 7.30 – 7.24 (m, 2H), 4.51 (t, *J* = 5.2 Hz, 1H), 4.31 – 4.20 (m, 1H), 3.36 (t, *J* = 5.4 Hz, 2H), 2.26–2.21 (m, 2H), 2.10 – 2.04 (m, 1H), 1.81 – 1.73 (m, 2H).

**Step 4: Synthesis of 4-fluoro-N-(3-formylcyclobutyl)benzamide:** To a 0 °C cooled suspension of 4-fluoro-N-(3-(hydroxymethyl)cyclobutyl)benzamide (1.2 g, 5.38 mmol, 1.0 equiv) in anhydrous DCM (30 mL) was added Dess-Martin periodinane (3.42 g, 8.06 mmol, 1.5 equiv) under nitrogen atmosphere and stirred at room temperature for 4 h. After completion of the reaction (monitored by TLC), the reaction mixture was cooled to 0 °C and quenched with aqueous 10% $NaHCO_3$ solution (30 mL) and extracted with DCM:methanol (9:1, 3 x 60 mL). The combined organic layers was dried over anhydrous $Na_2SO_4$ and concentrated under vacuum. The crude compound was purified by flash column chromatography (silica gel, 230-400 mesh) using 35 to 50% of ethyl acetate in petroleum ether as an eluent to afford 4-fluoro-N-(3-formylcyclobutyl)benzamide (0.86 g, 72.3%) as a white solid. MS (ESI positive ion) m/z: 222.0 (M+1). $^1$H NMR (400 MHz, DMSO-$d_6$) δ 9.64 (s, 1H), 8.69 (d, $J$ = 7.6 Hz, 1H), 7.94 – 7.90 (m, 2H), 7.32 – 7.27 (m, 2H), 4.49 – 4.40 (m, 1H), 3.02 – 2.93 (m, 1H), 2.44 – 2.37 (m, 2H), 2.29 – 2.22 (m, 2H).

**Step 5: Synthesis of N-(3-ethynylcyclobutyl)-4-fluorobenzamide:** To the solution of 4-fluoro-N-(3-formylcyclobutyl)benzamide (0.86 g, 3.89 mmol, 1.0 equiv) in anhydrous methanol (17 mL) was added anhydrous potassium carbonate (2.149 g, 15.55 mmol, 4 equiv) at room temperature under nitrogen atmosphere followed by dimethyl (1-diazo-2-oxopropyl)phosphonate (0.896 g, 4.66 mmol, 1.2 equiv) and stirred for 2 h. After completion of the reaction (indicated by TLC), reaction mixture was quenched with ice-cold water (35 mL) and extracted with 1:1 mixture of petroleum ether: ethyl acetate (3 x 20 mL). The combined organic layers was washed with brine (20 mL), dried over anhydrous $Na_2SO_4$ and concentrated under vacuum. The crude compound was purified by flash column chromatography (silica gel, 230-400 mesh) using 20 to 25% of ethyl acetate in petroleum ether as an eluent to afford N-(3-ethynylcyclobutyl)-4-

fluorobenzamide (0.465 g, 55.1%) as a white solid. MS (ESI positive ion) m/z: 218.0 (M+1). $^1$H NMR (400 MHz, DMSO-$d_6$) δ 7.79 – 7.76 (m, 2H), 7.15 – 7.10 (m, 2H), 6.21 (s, 1H), 4.58 – 4.45 (m, 1H), 2.89 – 2.76 (m, 3H), 2.34 (tdd, $J$ = 9.6, 7.6, 2.6 Hz, 1H), 2.11 (qd, $J$ = 8.9, 2.3 Hz, 2H).

**Step 6: Synthesis of N-(3-((2-bromophenyl)ethynyl)cyclobutyl)-4-fluorobenzamide:** To the mixture of N-(3-ethynylcyclobutyl)-4-fluorobenzamide (0.435 g, 2.002 mmol, 1.0 equiv), 1-bromo-2-iodobenzene (0.566 g, 0.680 mmol, 1.2 equiv), triphenylphosphine (0.026 g, 0.100 mmol, 0.05 equiv), bis(triphenylphosphine)palladium(II) chloride (0.070 g, 0.100 mmol, 0.05 equiv) and triethylamine (0.419 mL, 3.00 mmol, 1.5 equiv) was added anhydrous tetrahydrofuran (10 mL, degassed with nitrogen gas for 30 min) followed by copper (I) iodide (0.038 g, 0.200 mmol, 0.1 equiv) at room temperature under nitrogen atmosphere and stirred for 16 h. After completion of the reaction (monitored by TLC), water (10 mL) was added to the reaction mixture and extracted with ethyl acetate (3 x 5 mL). The combined organic layers were washed with brine (5 mL), dried over anhydrous $Na_2SO_4$ and concentrated under vacuum. The crude compound was purified by flash column chromatography (silica gel, 230-400 mesh) using 13 to 18% of ethyl acetate in petroleum ether as an eluent to afford N-(3-((2-bromophenyl)ethynyl)cyclobutyl)-4-fluorobenzamide (0.37 g, 49.6%) as a white solid. MS (ESI positive ion) m/z: 372.0, 374.0 (M, M+2). $^1$H NMR (300 MHz, Chloroform-$d$) δ 7.84 – 7.74 (m, 2H), 7.62 – 7.56 (m, 1H), 7.43 (dd, $J$ = 7.7, 1.8 Hz, 1H), 7.23 (dd, $J$ = 7.6, 1.3 Hz, 1H), 7.18 – 7.08 (m, 3H), 6.28 (s, 1H), 4.59 (q, $J$ = 8.2 Hz, 1H), 3.09 – 2.93 (m, 3H), 2.27 – 2.18 (m, 2H).

**Step 7: Synthesis of N-(3-((2-(2-amino-3-(3-((3,3-dimethylbutyl)amino)-3-oxopropyl)quinolin-6-yl)phenyl)ethynyl)cyclobutyl)-4-fluorobenzamide (Compound 7):** To

a solution of 3-(2-amino-6-(4,4,5,5-tetramethyl-1,3,2-dioxaborolan-2-yl)quinolin-3-yl)-N-(3,3-dimethylbutyl)propanamide (65 % purity, 175 mg, 0.267 mmol, 1.0 equiv) and N-(3-((2-bromophenyl)ethynyl)cyclobutyl)-4-fluorobenzamide (Step 6, 100 mg, 0.267 mmol, 1.0 equiv) taken in 1,4-dioxane (4 mL) and water (1 mL), was added sodium carbonate (56.7 mg, 0.535 mmol, 2.0 equiv), then degassed with nitrogen. Bis(triphenylphosphine)palladium (II) chloride (9.38 mg, 0.013 mmol, 0.05 equiv) was added at room temperature and then reaction mixture was stirred at 85 °C for 4 h. After completion of the reaction (monitored by TLC), the reaction mixture was quenched with water (5 mL) and extracted with ethyl acetate (2 x 20 mL). The organic extract was dried over $Na_2SO_4$ and concentrated in vacuo to give the crude material. The crude material was purified by flash column chromatography (silica gel, 230-400 mesh) eluting with a gradient of 0% to 30% methanol in chloroform, to provide 100 mg of the title product which was further purified by preparative HPLC [YMC C8 (20 x 250mm, 5μ); mobile phase: 10 mM $NH_4OAc$ in water and acetonitrile; flow rate: 18 mL/min]. After concentration the residue was taken in water and extracted with dichloromethane, the organic extract was dried over $Na_2SO_4$. The solution was filtered and concentrated in vacuo and the residue was washed with hexane and then lyophilized, to provide **Compound 7** (11 mg, 0.019 mmol, 6.96 % yield) as an off white solid. MS (ESI positive ion) m/z: 591.2 (M+1). $^1$H NMR (400 MHz, DMSO-$d_6$) δ 8.71 (d, $J$ = 7.6 Hz, 1H), 7.93 – 7.87 (m, 2H), 7.85 – 7.78 (m, 2H), 7.76 (s, 1H), 7.71 (dd, $J$ = 8.6, 2.2 Hz, 1H), 7.55 – 7.46 (m, 3H), 7.44 (dd, $J$ = 7.4, 1.5 Hz, 1H), 7.35 – 7.23 (m, 3H), 6.39 (s, 2H), 4.31 (d, $J$ = 7.9 Hz, 1H), 3.06 – 3.00 (m, 2H), 2.92 – 2.85 (m, 1H), 2.80 (t, $J$ = 7.4 Hz, 2H), 2.55 (t, $J$ = 1.9 Hz, 2H), 2.42 (d, $J$ = 7.5 Hz, 2H), 2.13 (q, $J$ = 10.3 Hz, 2H), 1.29 – 1.24 (m, 2H), 0.84 (s, 9H); $^{19}$F NMR (376 MHz, DMSO-$d_6$) δ -109.6.

**Synthesis of Compound 8.**

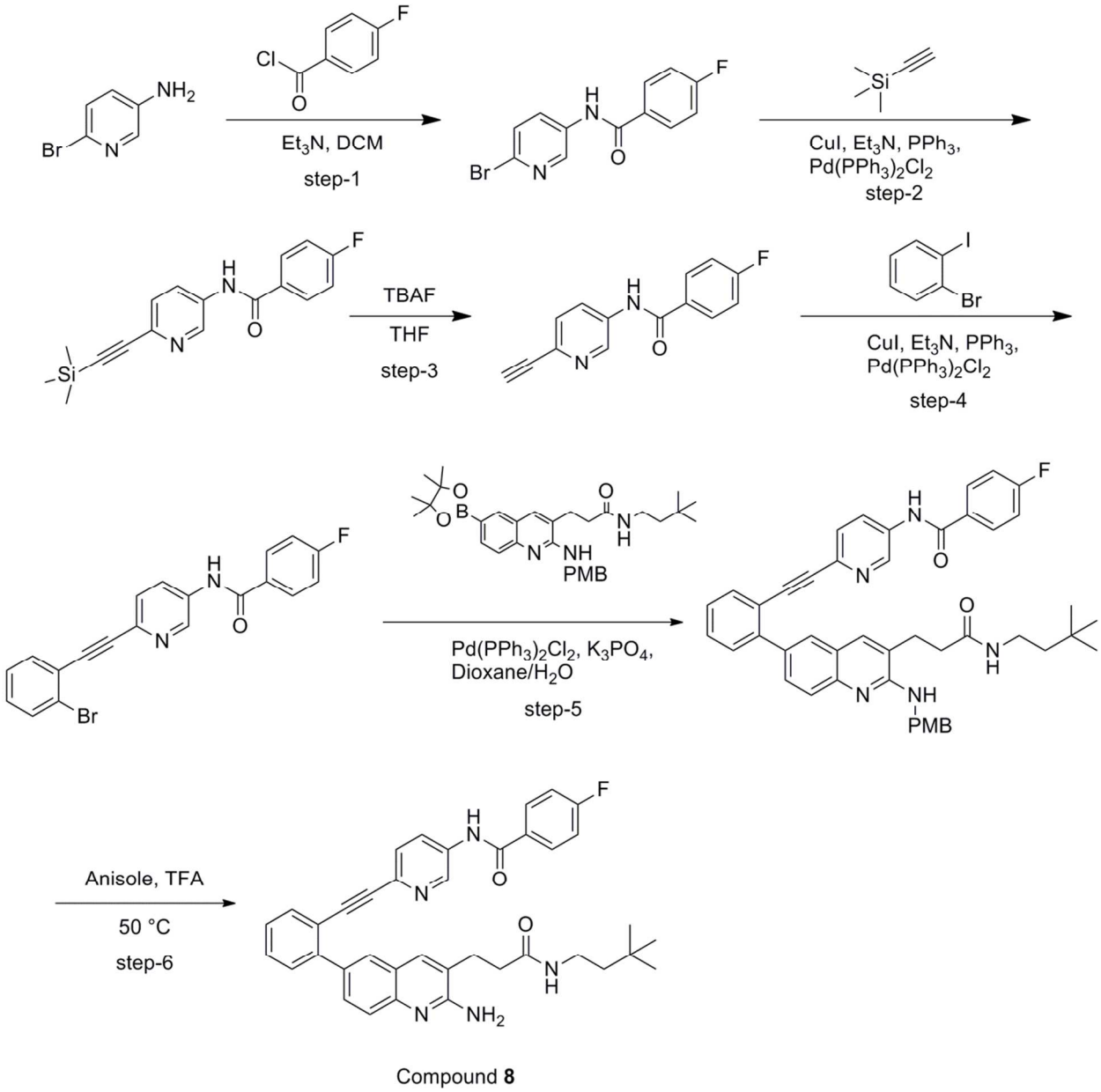


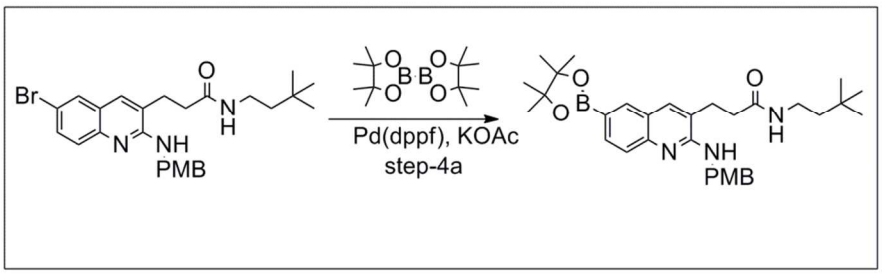

**Step 1: Synthesis of N-(6-bromopyridin-3-yl)-4-fluorobenzamide:** To the solution of 6-bromopyridin-3-amine (3 g, 17.34 mmol, 1.0 equiv) in anhydrous DCM (30 mL) was added triethylamine (3.63 mL, 26.0 mmol, 1.5 equiv) at room temperature under nitrogen atmosphere and cooled to 0 °C. 4-Fluorobenzoyl chloride (2.45 mL, 20.81 mmol, 1.2 equiv) was added dropwise to the above reaction mixture and stirred at room temperature for 5 h. After completion of the reaction (monitored by TLC), the reaction mixture was quenched with ice-cold water (30 mL) and separated the biphasic layers. The aqueous layer was extracted with DCM (30 mL). The combined organic layers were dried over anhydrous $Na_2SO_4$ and concentrated under vacuum to afford crude N-(6-bromopyridin-3-yl)-4-fluorobenzamide (5.25 g) as a brown solid. MS (ESI positive ion) m/z: 295.0, 297.0 (M, M+2). $^1$H NMR (400 MHz, Chloroform-*d*) δ 8.50 (s, 1H), 8.22 (ddd, *J* = 8.7, 3.1, 1.4 Hz, 1H), 7.94 – 7.88 (m, 3H), 7.52 (d, *J* = 8.6 Hz, 1H), 7.24 – 7.18 (m, 2H).

**Step 2: Synthesis of 4-fluoro-N-(6-((trimethylsilyl)ethynyl)pyridin-3-yl)benzamide:** To the mixture of N-(6-bromopyridin-3-yl)-4-fluorobenzamide (5.9 g, 19.99 mmol, 1.0 equiv), triphenylphosphine (0.262 g, 1.00 mmol, 0.05 equiv), bis(triphenylphosphine)palladium (II) chloride (0.702 g, 1.00 mmol, 0.05 equiv) and triethylamine (4.46 mL, 32.0 mmol, 1.6 equiv) was added anhydrous THF (120 mL, degassed with nitrogen gas for 30 min) and cooled to 0 °C. Trimethylsilylacetylene (4.21 mL, 30.0 mmol, 1.5 equiv) was added dropwise to the reaction mixture under nitrogen atmosphere followed by portion wise addition of copper (I) iodide (0.381 g, 1.99 mmol, 0.1 equiv) and stirred at room temperature for 16 h. After completion of the reaction (monitored by TLC), water (120 mL) was added to the reaction mixture and extracted with ethyl acetate (3 x 60 mL). The combined organic layers were washed with brine (60 mL),

dried over anhydrous $Na_2SO_4$ and concentrated under vacuum to afford crude N-(3-((2-bromophenyl)ethynyl)cyclobutyl)-4-fluorobenzamide (4.14 g) as a brown solid. MS (ESI positive ion) m/z: 313.2 (M+1).

**Step 3: Synthesis of N-(6-ethynylpyridin-3-yl)-4-fluorobenzamide:** To a solution of crude 4-fluoro-N-(6-((trimethylsilyl)ethynyl)pyridin-3-yl)benzamide (4.14 g, 13.25 mmol, 1.0 equiv) in anhydrous THF (20 mL) at 0 °C was added dropwise tetra-N-butylammonium fluoride (19.88 mL, 19.88 mmol, 1.5 equiv, 1.0 M solution in tetrahydrofuran) under nitrogen atmosphere and stirred at room temperature for 2 h. After completion of the reaction (monitored by TLC), reaction mixture was added ice-cold water (20 mL) and extracted with ethyl acetate (3 x 20 mL). The combined organic layers were washed with brine (20 mL), dried over anhydrous $Na_2SO_4$ and concentrated under vacuum. The crude compound was purified by flash column chromatography (silica gel, 230-400 mesh) using 30 to 45% of ethyl acetate in petroleum ether as an eluent to afford N-(6-ethynylpyridin-3-yl)-4-fluorobenzamide (0.77 g, 18% over two steps) as a pale brown solid. MS (ESI positive ion) m/z: 241.2 (M+1). $^1$H NMR (400 MHz, DMSO-$d_6$) δ 10.62 (s, 1H), 8.92 (d, $J$ = 2.5 Hz, 1H), 8.24 (dd, $J$ = 8.5, 2.4 Hz, 1H), 8.10 – 8.01 (m, 2H), 7.59 (d, $J$ = 8.5 Hz, 1H), 7.41 (tt, $J$ = 9.6, 2.5 Hz, 2H), 4.27 (s, 1H).

**Step 4: Synthesis of N-(6-((2-bromophenyl)ethynyl)pyridin-3-yl)-4-fluorobenzamide:** To the mixture of N-(6-ethynylpyridin-3-yl)-4-fluorobenzamide (0.77 g, 3.21 mmol, 1.0 equiv), 1-bromo-2-iodobenzene (1.088 g, 3.85 mmo, 1.2 equiv), triphenylphosphine (0.042 g, 0.160 mmol, 0.05 equiv), bis(triphenylphosphine)palladium (II) chloride (0.112 g, 0.160 mmol, 0.05 equiv) and triethylamine (0.67 mL, 4.81 mmol, 1.5 equiv) was added anhydrous tetrahydrofuran (15

mL, degassed with nitrogen gas for 30 min) followed by copper (I) iodide (0.061 g, 0.321 mmol, 0.1 equiv) at room temperature under nitrogen atmosphere and stirred for 4 h. After completion of the reaction (monitored by TLC), water (10 mL) was added to the reaction mixture and extracted with ethyl acetate (3 x 10 mL). The combined organic layers were washed with brine (10 mL), dried over anhydrous $Na_2SO_4$ and concentrated under vacuum. The crude compound was purified by flash column chromatography (silica gel, 230-400 mesh) using 25 to 30% of ethyl acetate in petroleum ether as an eluent to afford N-(6-((2-bromophenyl)ethynyl)pyridin-3-yl)-4-fluorobenzamide (0.56 g, 44.2%) as yellow solid. MS (ESI positive ion) m/z: 395.0, 397.0 (M, M+2). $^1$H NMR (400 MHz, Chloroform-*d*) δ 8.77 (d, *J* = 2.6 Hz, 1H), 8.45 (dd, *J* = 8.6, 2.6 Hz, 1H), 8.32 (s, 1H), 7.97 (ddd, *J* = 8.7, 5.2, 2.5 Hz, 2H), 7.67 – 7.58 (m, 3H), 7.31 (dd, *J* = 7.4, 1.3 Hz, 1H), 7.26 – 7.16 (m, 3H).

**Step 4a: Synthesis of N-(3,3-dimethylbutyl)-3-(2-((4-methoxybenzyl)amino)-6-(4,4,5,5-tetramethyl-1,3,2-dioxaborolan-2-yl)quinolin-3-yl)propanamide:** To a solution of 3-(6-bromo-2-((4-methoxybenzyl)amino)quinolin-3-yl)-N-(3,3-dimethylbutyl)propanamide (1 g, 2.006 mmol, 1.0 equiv) in 1,4-dioxane (20 mL), was added potassium acetate (0.591 g, 6.02 mmol, 3.0 equiv) and bis(pinacolato)diboron (0.611 g, 2.407 mmol, 1.2 equiv), then degassed with nitrogen and then added $PdCl_2$(dppf)-$CH_2Cl_2$ (0.082 g, 0.100 μmol, 0.05 equiv) at room temperature. The reaction mixture was stirred at 85 °C for 16 h. After completion of the reaction (monitored by TLC), the mixture was quenched with water (20 mL) and extracted with ethyl acetate (2 x 25 mL). The organic layer was washed with brine (15 mL) and dried over $Na_2SO_4$. The solution was filtered and concentrated in vacuo to give the crude material which was passed through a bed of silica gel for removing of inorganics, to provide N-(3,3-dimethylbutyl)-3-(2-((4-

methoxybenzyl)amino)-6-(4,4,5,5-tetramethyl-1,3,2-dioxaborolan-2-yl)quinolin-3-yl)propanamide (1 g, 1.833 mmol, 91 % yield), as a brown solid. MS (ESI positive ion) m/z: 546.2 (M +1).

**Step 5: Synthesis of N-(6-((2-(3-(3-((3,3-dimethylbutyl)amino)-3-oxopropyl)-2-((4-methoxybenzyl)amino)quinolin-6-yl)phenyl)ethynyl)pyridin-3-yl)-4-fluorobenzamide:** To the solution of crude N-(3,3-dimethylbutyl)-3-(2-((4-methoxybenzyl)amino)-6-(4,4,5,5-tetramethyl-1,3,2-dioxaborolan-2-yl)quinolin-3-yl)propanamide (0.350 g, 0.642 mmol, 1.0 equiv) in 1,4-dioxane (6 mL) and water (2 mL) was added N-(6-((2-bromophenyl)ethynyl)pyridin-3-yl)-4-fluorobenzamide (0.254 g, 0.642 mmol, 1.0 equiv) followed by potassium phosphate tribasic (0.340 g, 1.604 mmol, 2.5 equiv) at room temperature and purged with nitrogen gas for 30 min. Bis(triphenylphosphine)palladium(ii) chloride (0.023 g, 0.032 mmol, 0.05 equiv) was added to the reaction mixture and heated to 110 °C for 36 h. After completion of the reaction (monitored by TLC), reaction mixture was cooled to room temperature, added water (10 mL) and extracted with ethyl acetate (2 x 10 mL). The combined organic layers were washed with brine (10 mL), dried over anhydrous $Na_2SO_4$ and concentrated under vacuum. The crude compound was purified by flash column chromatography (silica gel, 230-400 mesh) using 45 to 60% of ethyl acetate in petroleum ether as an eluent to afford N-(6-((2-(3-(3-((3,3-dimethylbutyl)amino)-3-oxopropyl)-2-((4-methoxybenzyl)amino)quinolin-6-yl)phenyl)ethynyl)pyridin-3-yl)-4-fluorobenzamide (0.20 g, 70% pure, 29.7%) as a brown solid. MS (ESI negative ion) m/z: 732.0 (M-1). $^1$H NMR (400 MHz, Chloroform-*d*) δ 8.71 (s, 1H), 8.19 (d, *J* = 8.6 Hz, 1H), 8.03 (s, 1H), 7.97 (t, *J* = 6.8 Hz, 2H), 7.82 (d, *J* = 8.6 Hz, 1H), 7.75 – 7.60 (m, 4H), 7.57 – 7.39 (m, 6H), 7.34 – 7.31 (m, 1H), 7.12 (d, *J* = 8.6 Hz, 3H), 6.86 (d, *J* = 8.1

Hz, 2H), 4.79 (d, *J* = 5.1 Hz, 2H), 3.78 (d, *J* = 1.8 Hz, 3H), 3.25 – 3.16 (m, 2H), 2.94 (t, *J* = 7.4 Hz, 2H), 1.35 – 1.25 (m, 4H), 0.84 (d, *J* = 1.7 Hz, 9H).

**Step 6: Synthesis of N-(6-((2-(2-amino-3-(3-((3,3-dimethylbutyl)amino)-3-oxopropyl)quinolin-6-yl)phenyl)ethynyl)pyridin-3-yl)-4-fluorobenzamide (Compound 8):** To a mixture of N-(6-((2-(3-(3-((3,3-dimethylbutyl)amino)-3-oxopropyl)-2-((4-methoxybenzyl)amino)quinolin-6-yl)phenyl)ethynyl)pyridin-3-yl)-4-fluorobenzamide (0.050 g, 0.068 mmol, 1.0 equiv) and anisole (0.074 g, 0.681 mmol, 10 equiv) at 0 °C was added TFA (2 mL) under nitrogen atmosphere and heated to 50 °C for 2 h. After completion of the reaction (monitored by TLC), reaction mixture was cooled to room temperature and concentrated under vacuum. Aqueous 10% $NaHCO_3$ solution (5 mL) was added to the reaction mixture (upto reach ~pH-7) followed by ethyl acetate (5 mL) and stirred for 15 min. The biphasic layers were separated and the aqueous layer was extracted with ethyl acetate (3 x 5 mL). The combined organic layers were washed with brine (5 mL), dried over anhydrous $Na_2SO_4$ and concentrated under vacuum. The crude compound was purified by flash column chromatography (silica gel, 230-400 mesh) using 5 to 6% of methanol in DCM as an eluent to afford N-(6-((2-(2-amino-3-(3-((3,3-dimethylbutyl)amino)-3-oxopropyl)quinolin-6-yl)phenyl)ethynyl)pyridin-3-yl)-4-fluorobenzamide (**Compound 8**, 0.029 g, 69.4%) as a pale yellow solid. MS (ESI positive ion) m/z: 614.0 (M+1). $^1$H NMR (400 MHz, DMSO-$d_6$) δ 10.61 (s, 1H), 8.90 (d, *J* = 2.5 Hz, 1H), 8.22 (dd, *J* = 8.6, 2.6 Hz, 1H), 8.10 – 8.03 (m, 2H), 7.92 (d, *J* = 2.1 Hz, 1H), 7.89 – 7.75 (m, 3H), 7.73 (d, *J* = 7.7 Hz, 1H), 7.65 – 7.51 (m, 3H), 7.50 – 7.33 (m, 4H), 6.65 (s, 2H), 3.08 – 2.99 (m, 2H), 2.85 (t, *J* = 7.3 Hz, 2H), 2.44 (t, *J* = 7.3 Hz, 2H), 1.28 – 1.22 (m, 2H), 0.81 (s, 9H); $^{19}$F NMR (376 MHz, DMSO-$d_6$) δ -109.4.

**Synthesis of Compound 9 (continued from synthesis of compound 8):**

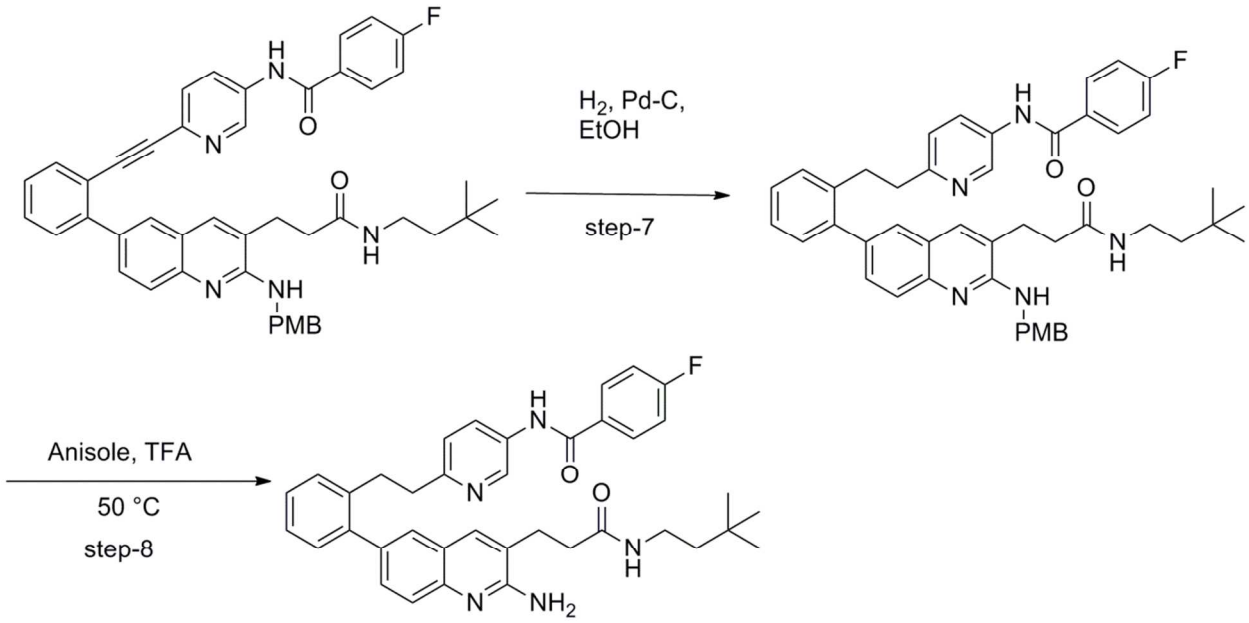


Compound **9**

**Step 7: Synthesis of N-(6-(2-(3-(3-((3,3-dimethylbutyl)amino)-3-oxopropyl)-2-((4-methoxybenzyl)amino)quinolin-6-yl)phenethyl)pyridin-3-yl)-4-fluorobenzamide:** To the solution of N-(6-((2-(3-(3-((3,3-dimethylbutyl)amino)-3-oxopropyl)-2-((4-methoxybenzyl)amino)quinolin-6-yl)phenyl)ethynyl)pyridin-3-yl)-4-fluorobenzamide (0.050 g, 0.068 mmol, 1.0 equiv) in anhydrous ethanol (5 mL) was added 10% palladium on carbon (10 mg, 20 wt%) at room temperature and stirred under hydrogen pressure (15 psi) for 48 h. After completion of the reaction (monitored by TLC & HPLC), reaction mixture was filtered through a pad of celite, washed with ethanol (4 x 2 mL) and concentrated under vacuum to yield N-(6-(2-(3-(3-((3,3-dimethylbutyl)amino)-3-oxopropyl)-2-((4-methoxybenzyl)amino)quinolin-6-yl)phenethyl)pyridin-3-yl)-4-fluorobenzamide (0.04 g, 80%) as yellow solid. MS (ESI positive ion) m/z: 738.2 (M+1). $^1$H NMR (400 MHz, DMSO-$d_6$) δ 10.36 (s, 1H), 8.74 – 8.70 (m, 1H), 8.06 – 8.02 (m, 2H), 7.97 (dd, $J$ = 8.4, 2.6 Hz, 1H), 7.83 (t, $J$ = 5.4 Hz, 1H), 7.70 (s, 1H), 7.67 –

7.51 (m, 6H), 7.40 – 7.34 (m, 3H), 7.32 – 7.13 (m, 3H), 7.00 (d, *J* = 8.4 Hz, 1H), 6.89 – 6.84 (m, 2H), 4.66 (d, *J* = 5.7 Hz, 2H), 3.71 (s, 3H), 3.09 – 3.02 (m, 2H), 2.99 – 2.94 (m, 2H), 2.89 – 2.83 (m, 4H), 1.29 – 1.21 (m, 4H), 0.83 (s, 9H).

**Step 8: Synthesis of N-(6-(2-(2-amino-3-(3-((3,3-dimethylbutyl)amino)-3-oxopropyl)quinolin-6-yl)phenethyl)pyridin-3-yl)-4-fluorobenzamide TFA (Compound 9):** To a mixture of N-(6-(2-(3-(3-((3,3-dimethylbutyl)amino)-3-oxopropyl)-2-((4-methoxybenzyl)amino)quinolin-6-yl)phenethyl)pyridin-3-yl)-4-fluorobenzamide (0.045 g, 0.061 mmol, 1.0 equiv) and anisole (0.066 g, 0.610 mmol, 10 equiv) at 0 °C was added TFA (2 mL) under nitrogen atmosphere and heated to 50 °C for 3 h. After completion of the reaction (monitored by TLC), the reaction mixture was cooled to room temperature and concentrated under vacuum. Aqueous 10% $NaHCO_3$ solution (5 mL) was added to the reaction mixture (up to ~pH-7) followed by ethyl acetate (5 mL) and stirred for 15 min. The biphasic layers were separated and the aqueous layer was extracted with ethyl acetate (3 x 5 mL). The combined organic layers were washed with brine (5 mL), dried over anhydrous $Na_2SO_4$ and concentrated under vacuum. The crude compound was purified by flash column chromatography (silica gel, 230-400 mesh) using 5 to 6% of methanol in DCM as an eluent to yield the desired crude product (0.034 g, 91%) which was further purified by preparative HPLC (Chromosil-C18; mobile phase: 10 mM $NH_4OAc$ in water and acetonitrile; flow rate: 18 mL/min; peak RT: 16.1 min] and after partial concentration, the material was extracted from the aqueous layer (~10 mL) with DCM (3 x 5 mL). The combined organic layers was washed with brine (5 mL), dried over anhydrous $Na_2SO_4$ and concentrated under vacuum to yield N-(6-(2-(2-amino-3-(3-((3,3-dimethylbutyl)amino)-3-oxopropyl)quinolin-6-yl)phenethyl)pyridin-3-yl)-4-fluorobenzamide (Compound **9**) as a TFA salt (0.015 g, 39.8%, white solid). MS (ESI positive ion) m/z: 618.2

(M+1). $^{1}$H NMR (400 MHz, DMSO-$d_6$) δ 10.36 (s, 1H), 8.71 (d, $J$ = 2.6 Hz, 1H), 8.07 – 8.01 (m, 2H), 7.97 (dd, $J$ = 8.4, 2.6 Hz, 1H), 7.83 (t, $J$ = 5.5 Hz, 1H), 7.74 (s, 1H), 7.54 – 7.46 (m, 2H), 7.43 – 7.35 (m, 4H), 7.33 – 7.19 (m, 3H), 6.99 (d, $J$ = 8.4 Hz, 1H), 6.45 (s, 2H), 3.08 – 2.93 (m, 4H), 2.91 – 2.76 (m, 4H), 2.43 (t, $J$ = 7.4 Hz, 2H), 1.29 – 1.24 (m, 2H), 0.82 (s, 9H); $^{19}$F NMR (376 MHz, DMSO-$d_6$) δ -73.4, -108.5.

**Supporting Information.** Table of crystallographic data, SPR sensorgrams, BACE-1, BACE-2, and CatD enzyme assay data. This material is available free of charge via the Internet at http://pubs.acs.org.

**Accession Codes**

New protein/ligand coordinates have been deposited in the PDB with IDs of 5I3V, 5I3W, 5I3X, 5I3Y, 5IE1.

**Corresponding Author Information:** Brad Jordan, Ph.D., 805-313-5647 (phone), brad.jordan@amgen.com.

**Acknowledgements:** The authors would like to thank Alexander M. Long for purification of BACE-1 protein. X-ray diffraction data were collected at the Advanced Light Source, which is supported by the U. S. Department of Energy, Office of Science, Office of Basic Energy Sciences under Contract No. DE-AC02-05CH11231. Diffraction data were also collected at Southeast Regional Collaborative Access Team (SER-CAT) beamline 22-BM at the Advanced Photon Source of Argonne National Laboratory. Use of the Advanced Photon Source was

supported by the U. S. Department of Energy, Office of Science, Office of Basic Energy Sciences, under Contract No. W-3-109-Eng-38.

**Abbreviations Used**: FBDD, Fragment Based Drug Discovery; FBS, Fragment Based Screening; CatD, Cathepsin-D; BACE-1, □-Site APP Cleaving Enzyme-1; LE, Ligand Efficiency; HA, Heavy Atoms; HTS, High Throughput Screening; NMR, Nuclear Magnetic Resonance; SPR, Surface Plasmon Resonance; ILNOE, Inter-ligand Nuclear Overhauser Enhancement; NOESY, Nuclear Overhauser Enhancement Spectroscopy; STD, Saturation Transfer Difference; WaterLOGSY, Water-Ligand Observe Gradient SpectroscopY; SAR, Structure Activity Relationship; TBDMS-Cl, tert-butyldimethylsilyl chloride; TLC, thin-layer chromatography; DCM, dichloromethane;

## References

1. Baker, M. Fragment-based lead discovery grows up. *Nat. Rev. Drug Discovery* **2013,** 12, 5-7.

2. Shuker, S. B.; Hajduk, P. J.; Meadows, R. P.; Fesik, S. W. Discovering high-affinity ligands for proteins: SAR by NMR. *Science* **1996**, *274*, 1531-1534.

3. Mayer, M.; Meyer, B. Characterization of ligand binding by saturation transfer difference NMR spectroscopy. *Angew. Chem.* **1999**, *38*, 1784-1788.

4. Dalvit, C.; Fagerness, P. E.; Hadden, D. T.; Sarver, R. W.; Stockman, B. J. Fluorine-NMR experiments for high-throughput screening: theoretical aspects, practical considerations, and range of applicability. *J. Am. Chem. Soc.* **2003**, *125*, 7696-7703.

5. Jordan, J. B.; Poppe, L.; Xia, X.; Cheng, A. C.; Sun, Y.; Michelsen, K.; Eastwood, H.; Schnier, P. D.; Nixey, T.; Zhong, W. Fragment based drug discovery: practical implementation based on (1)(9)F NMR spectroscopy. *J. Med. Chem.* **2012**, *55*, 678-687.

6. Vulpetti, A.; Hommel, U.; Landrum, G.; Lewis, R.; Dalvit, C. Design and NMR-based screening of LEF, a library of chemical fragments with different local environment of fluorine. *J. Am. Chem. Soc.* **2009**, *131*, 12949-12959.

7. Poppe, L.; Harvey, T. S.; Mohr, C.; Zondlo, J.; Tegley, C. M.; Nuanmanee, O.; Cheetham, J. Discovery of ligands for Nurr1 by combined use of NMR screening with different isotopic and spin-labeling strategies. *J. Biomol. Screening* **2007**, *12*, 301-311.

8. Querfurth, H. W.; LaFerla, F. M. Alzheimer's disease. *N. Engl. J. Med.* **2010**, 362, 329-344.

9. Hardy, J.; Selkoe, D. J. The amyloid hypothesis of Alzheimer's disease: progress and problems on the road to therapeutics. *Science* **2002**, *297,* 353-356.

10. De Strooper, B.; Vassar, R.; Golde, T. The secretases: enzymes with therapeutic potential in Alzheimer disease. *Nat. Rev. Neurol.* **2010**, *6*, 99-107.

11. Vassar, R.; Bennett, B. D.; Babu-Khan, S.; Kahn, S.; Mendiaz, E. A.; Denis, P.; Teplow, D. B.; Ross, S.; Amarante, P.; Loeloff, R.; Luo, Y.; Fisher, S.; Fuller, J.; Edenson, S.; Lile, J.; Jarosinski, M. A.; Biere, A. L.; Curran, E.; Burgess, T.; Louis, J. C.; Collins, F.; Treanor, J.; Rogers, G.; Citron, M. Beta-secretase cleavage of Alzheimer's amyloid precursor protein by the transmembrane aspartic protease BACE. *Science* **1999**, *286*, 735-741.

12. Murray, C. W.; Callaghan, O.; Chessari, G.; Cleasby, A.; Congreve, M.; Frederickson, M.; Hartshorn, M. J.; McMenamin, R.; Patel, S.; Wallis, N. Application of fragment screening by X-ray crystallography to beta-secretase. *J. Med. Chem.* **2007**, *50*, 1116-1123.

13. Cheng, Y.; Judd, T. C.; Bartberger, M. D.; Brown, J.; Chen, K.; Fremeau, R. T., Jr.; Hickman, D.; Hitchcock, S. A.; Jordan, B.; Li, V.; Lopez, P.; Louie, S. W.; Luo, Y.; Michelsen, K.; Nixey, T.; Powers, T. S.; Rattan, C.; Sickmier, E. A.; St Jean, D. J., Jr.; Wahl, R. C.; Wen, P. H.; Wood, S. From fragment screening to in vivo efficacy: optimization of a series of 2-aminoquinolines as potent inhibitors of beta-site amyloid precursor protein cleaving enzyme 1 (BACE1). *J. Med. Chem.* **2011**, *54*, 5836-5857.

14. Congreve, M.; Aharony, D.; Albert, J.; Callaghan, O.; Campbell, J.; Carr, R. A.; Chessari, G.; Cowan, S.; Edwards, P. D.; Frederickson, M.; McMenamin, R.; Murray, C. W.; Patel, S.; Wallis, N. Application of fragment screening by X-ray crystallography to the discovery of aminopyridines as inhibitors of beta-secretase. *J. Med. Chem.* **2007**, *50*, 1124-1132.

15. Stamford, A.; Strickland, C. Inhibitors of BACE for treating Alzheimer's disease: a fragment-based drug discovery story. *Curr. Opin. Chem. Biol.* **2013**, *17*, 320-328.

16. Wyss, D. F.; Wang, Y. S.; Eaton, H. L.; Strickland, C.; Voigt, J. H.; Zhu, Z.; Stamford, A. W. Combining NMR and X-ray crystallography in fragment-based drug discovery: discovery of highly potent and selective BACE-1 inhibitors. *Top. Curr. Chem.* **2012**, *317*, 83-114.

17. Huang, H.; La, D. S.; Cheng, A. C.; Whittington, D. A.; Patel, V. F.; Chen, K.; Dineen, T. A.; Epstein, O.; Graceffa, R.; Hickman, D.; Kiang, Y. H.; Louie, S.; Luo, Y.; Wahl, R. C.; Wen, P. H.; Wood, S.; Fremeau, R. T., Jr. Structure- and property-based design of aminooxazoline xanthenes as selective, orally efficacious, and CNS penetrable BACE inhibitors for the treatment of Alzheimer's disease. *J. Med. Chem.* **2012**, *55,* 9156-9169.

18. Steinfeld, R.; Reinhardt, K.; Schreiber, K.; Hillebrand, M.; Kraetzner, R.; Bruck, W.; Saftig, P.; Gartner, J. Cathepsin D deficiency is associated with a human neurodegenerative disorder. *Am. J. Hum. Genet.* **2006**, *78*, 988-998.

19. Bjorklund, C.; Oscarson, S.; Benkestock, K.; Borkakoti, N.; Jansson, K.; Lindberg, J.; Vrang, L.; Hallberg, A.; Rosenquist, A.; Samuelsson, B. Design and synthesis of potent and selective BACE-1 inhibitors. *J. Med. Chem.* **2010**, *53*, 1458-1464.

20. Page, M. I.; Jencks, W. P. Entropic contributions to rate accelerations in enzymic and intramolecular reactions and the chelate effect. *Proc. Natl. Acad. Sci. U.S.A.* **1971**, *68,* 1678-1683.

21. Jencks, W. P. On the attribution and additivity of binding energies. *Proc. Natl. Acad. Sci. U.S.A.* **1981**, *78*, 4046-4050.

22. Hajduk, P. J.; Huth, J. R.; Sun, C. SAR by NMR: An Analysis of Potency Gains Realized Through Fragment-linking and Fragment-elaboration Strategies for Lead Generation. In *Fragment-based Apporaches in Drug Discovery*, Erlanson, D. A., Jahnke, W., Ed. Wiley-VCH: Weinheim, 2006; pp 181-192.

23. Murray, C. W.; Verdonk, M. L. The consequences of translational and rotational entropy lost by small molecules on binding to proteins. *J. Comput.-Aided Mol. Des.* **2002**, *16*, 741-753.

24. Davies, T. G., Monfort, R.L.M., Williams, G., Jhoti, H. Pyramid: An integrated platform for fragment-based drug discovery. In *Fragment-based Approaches in Drug Discovery*, Erlanson, D. A., Jahnke, W., Ed. Oxford University Press: Oxford, UK, 2006.

25. Li, D.; DeRose, E. F.; London, R. E. The inter-ligand Overhauser effect: a powerful new NMR approach for mapping structural relationships of macromolecular ligands. *J. Biomol. NMR* **1999**, *15*, 71-76.

26. *Molecular Operating Environment*, Chemical Computing Group: Montreal, Canada, 2012.

27. Case, D. A.; Cheatham, T. E., 3rd; Darden, T.; Gohlke, H.; Luo, R.; Merz, K. M., Jr.; Onufriev, A.; Simmerling, C.; Wang, B.; Woods, R. J. The Amber biomolecular simulation programs. *J. Comput. Chem.* **2005**, *26,* 1668-1688.

28. Patel, S.; Vuillard, L.; Cleasby, A.; Murray, C. W.; Yon, J. Apo and inhibitor complex structures of BACE (beta-secretase). *J. Mol. Biol.* **2004**, *343*, 407-416.

29. Otwinowski, Z., Minor, W. Processing of X-ray Diffraction Data Collected in Oscillation Mode. In *Methods in Enzymology*, Academic Press: New York, 1997; Vol. 276, pp 307-326.

30. Murshudov, G. N.; Vagin, A. A.; Dodson, E. J. Refinement of macromolecular structures by the maximum-likelihood method. *Acta. Crystallogr., Sect. D: Biol. Crystallogr.* **1997**, *53*, 240-255.

31. Emsley, P.; Cowtan, K. Coot: model-building tools for molecular graphics. *Acta. Crystallogr.,Sect D: Biol. Crystallogr.* **2004**, *60*, 2126-2132.

32. Turner, R. T., 3rd; Koelsch, G.; Hong, L.; Castanheira, P.; Ermolieff, J.; Ghosh, A. K.; Tang, J. Subsite specificity of memapsin 2 (beta-secretase): implications for inhibitor design. *Biochemistry* **2001**, *40*, 10001-10006.

33. Haniu, M.; Denis, P.; Young, Y.; Mendiaz, E. A.; Fuller, J.; Hui, J. O.; Bennett, B. D.; Kahn, S.; Ross, S.; Burgess, T.; Katta, V.; Rogers, G.; Vassar, R.; Citron, M. Characterization of Alzheimer's beta -secretase protein BACE. A pepsin family member with unusual properties. *J. Biol. Chem.* **2000**, *275*, 21099-21106.

**Figure 1**

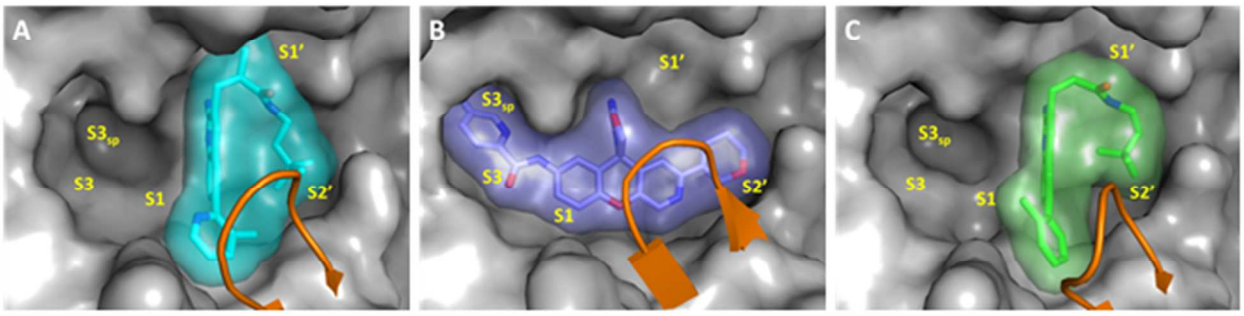


**Figure 1.** (A) X-ray crystal structure of BACE-1 in complex with the blocking compound **1** (PDB ID 5I3V) used in the study. Notice that the binding site of the protein is largely occupied while leaving S3 and $S3_{subpocket\ (sp)}$ accessible to fragments. (B) X-ray crystal structure of BACE-1 in complex with competitor compound **2** (PDB ID 5I3W) that occupies the $S3_{sp}$.(C) X-ray crystal structure of BACE-1 in complex with compound **5** (PDB ID 5IE1) to which the $^{19}F$ fragment (compound **3**) was linked. Notice that the toluyl methyl group in compound **5** points directly toward the S3 pocket.

Figure 2

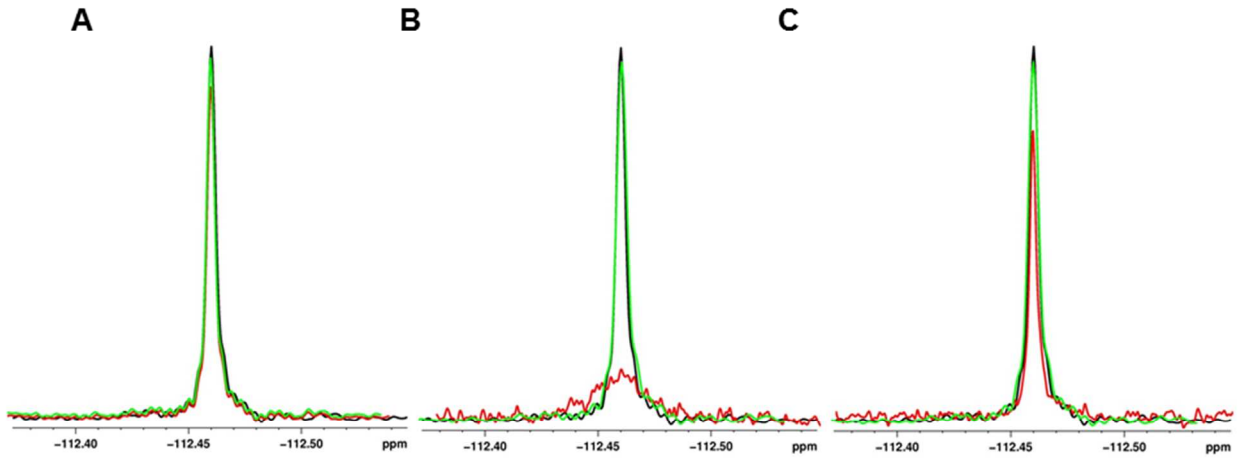


**Figure 2**. $^{19}$F NMR data of the best hit (compound **3**) from the fragment screen. **A)** NMR spectra of the free ligand (black) and the fragment in the presence of BACE-1(red) and in the presence of CatD (green). No binding to either protein is observed. **B)** NMR spectra of the free fragment (black) and the fragment in the presence of BACE-1 and CatD along with saturating concentrations of compound **1** (red and green, respectively). Binding of the fragment to BACE-1 is exhibited by broadening of the NMR signal, demonstrating that the fragment only binds in the presence of the blocking compound. The signal exhibits no change with CatD, indicating a lack of binding. **C)** NMR spectra of the free fragment (black) and the fragment in the presence of BACE-1 and CatD, the blocking compound, and 2 μM of the competitor ligand (compound **2**, red and green, respectively). The sharpening of the NMR signal indicates that the newly added ligand competes out the binding fragment, thus suggesting that the fragment likely binds to the S3 pocket of BACE-1.

Figure 3

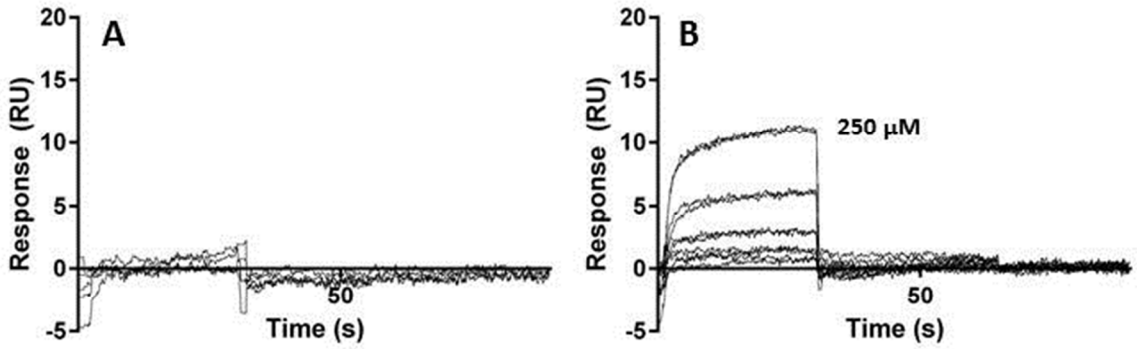


**Figure 3.** SPR sensorgrams of the lead $^{19}F$ fragment hit (compound **3**) binding to BACE-1 in the A) absence of blocking compound (no binding observed) and B) in the presence of saturating concentrations of the blocking compound (compound **1**, 5 μM). $K_D$ values were obtained using steady-state analysis and fitting to a global $R_{max}$ determined using a control compound. Sensorgrams shown are the same experiments run in duplicate.

Figure 4

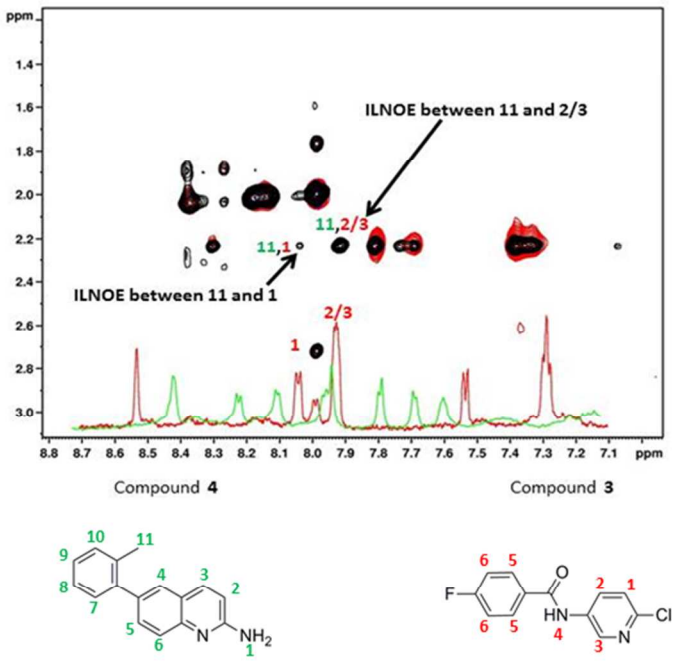


**Figure 4.** Transfer NOE experiments using compound **3** and compound **4**. NOEs are present between the number 11 proton of compound **4** and the number 1 and 2/3 protons of compound **3**. Green peaks are from compound **4** alone, red peaks are from compound **3** alone, and black peaks are from the mixture of compound **3** and compound **4**. Peaks present in the mixture spectrum (black) that are not present in the other two spectra are inter-ligand NOEs between compound **3** and **4**.

Figure 5.

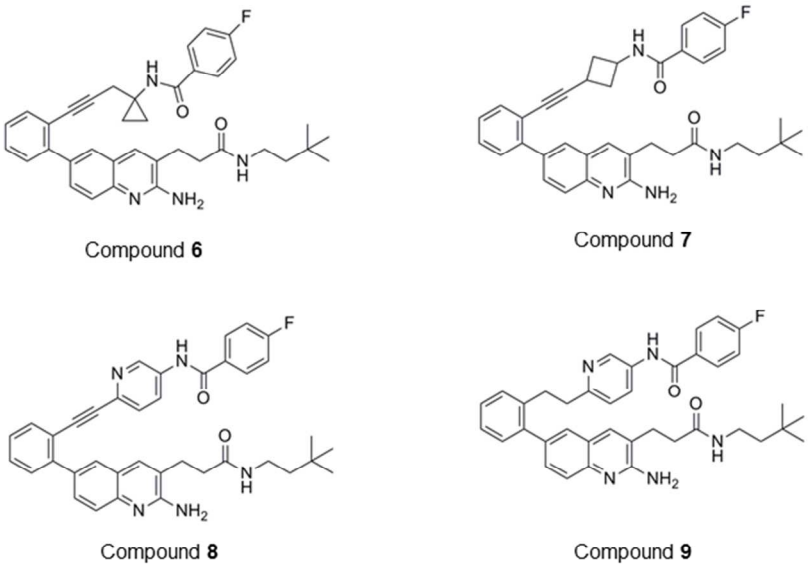


**Figure 5.** Proposed fragment-linked compounds derived from molecular modeling and ILNOE NMR experiments.

Figure 6.

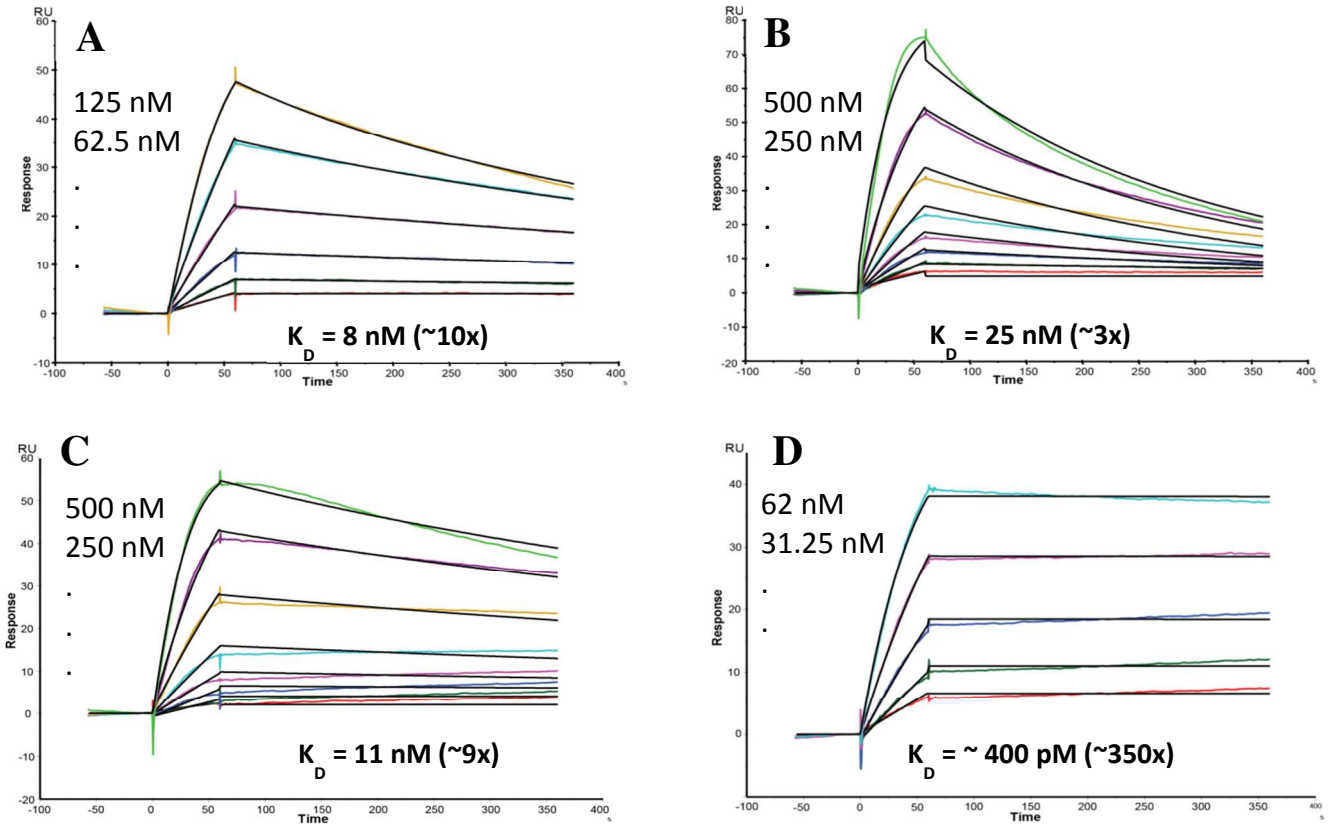


**Figure 6.** SPR binding experiments to BACE-1 of A) compound **6**, B) compound **7**, C) compound **8**, and D) compound **9**. Reported $K_D$ values are the average of two experiments and the values in parentheses denote the fold increase in affinity over the parent molecule (compound **5**).

Figure 7.

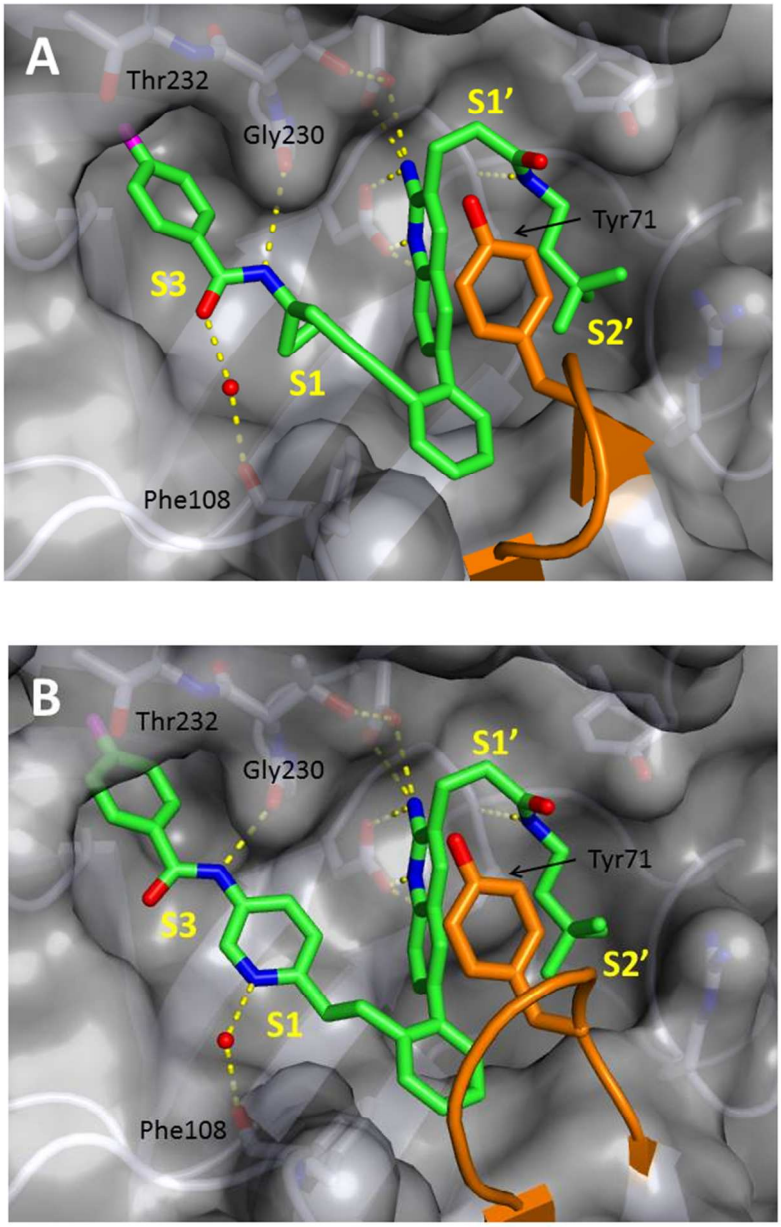


**Figure 7.** Co-crystal structures of small molecule ligands in complex with BACE-1. A) Compound **6** and B) compound **9**. Notice that the fluorphenyl group of compound **9** extends deep into the $S3_{subpocket}$, providing additional potency against BACE-1 and additional selectivity against CatD.

**Table 1.**

| Compound | Structure | $K_{D,SPR}$ BACE | LE[a] | $IC_{50,CatD}$ | MW (Da) |
|---|---|---|---|---|---|
| **1** | 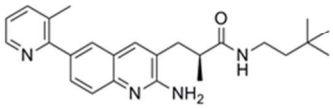 | 16 nM | 0.37 | 820 nM | 404.5 |
| **2** | 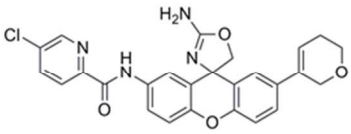 | 0.6 nM | 0.37 | 470 µM | 489.9 |
| **3** | 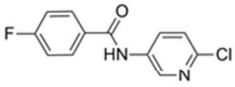 | 114 µM | 0.24 | ND | 250.6 |
| **4** | 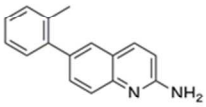 | 20 µM | 0.28 | 108 µM | 234.3 |
| **5** | 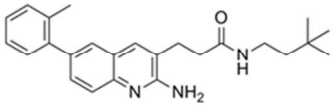 | 140 nM | 0.33 | 510 nM | 389.5 |

[a] Ligand efficiency calculated from SPR $K_D$ value

**Table 2:**

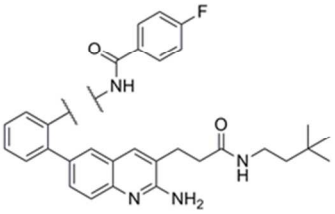

| Compound | Structure | $K_{D,SPR}$ BACE[a] | LE[b] | $IC_{50,enzyme}$ BACE [a] | CatD[a] | $IC_{50,cell}$ /Cell Shift[a] | cLogP[c] |
|---|---|---|---|---|---|---|---|
| **6** |  | 8 | 0.26 | 9 | 99 | 191/24 | 7.01 |
| **7** |  | 25 | 0.24 | 28 | 197 | 1000/36 | 7.05 |
| **8** | 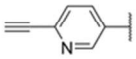 | 11 | 0.24 | 14 | 58 | 458/33 | 7.24 |
| **9** | 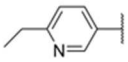 | 0.4 | 0.28 | 0.8 | 1900 | 16/20 | 7.67 |

[a]All values reported in nanomolar. [b] Ligand efficiency values calculated using $K_D$ from SPR. [c] cLogP values calculated using ChemBioDraw Ultra ®.

TOC Graphic

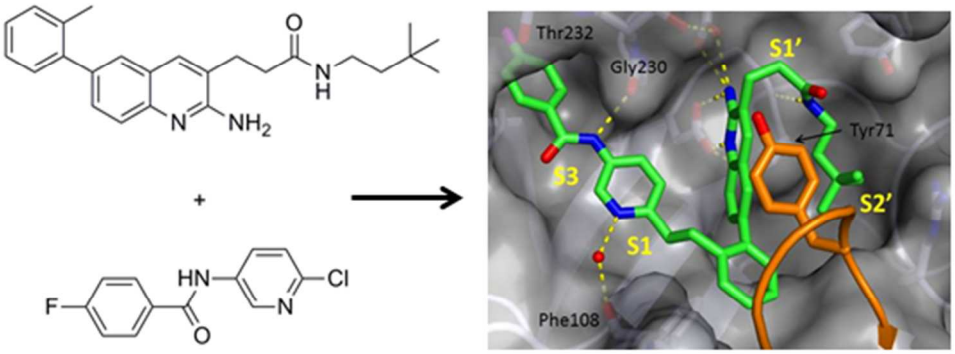

Figure 1

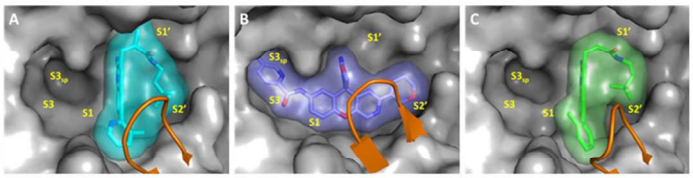


254x190mm (96 x 96 DPI)

Figure 2

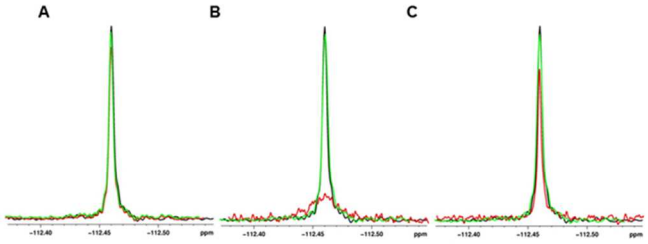


254x190mm (96 x 96 DPI)

Figure 3

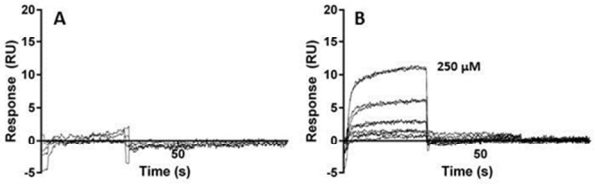


254x190mm (96 x 96 DPI)

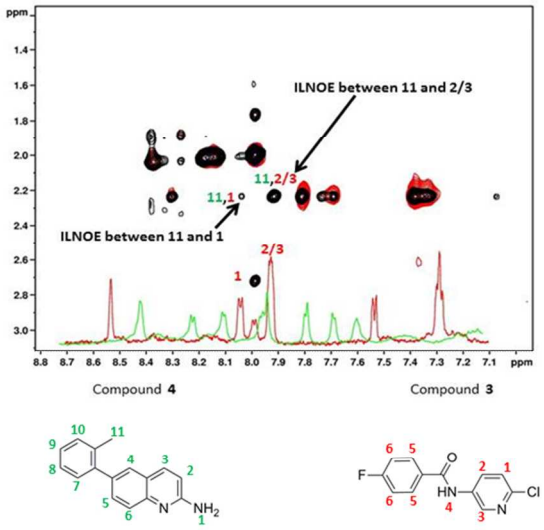


Figure 4.
254x190mm (96 x 96 DPI)

Figure 6

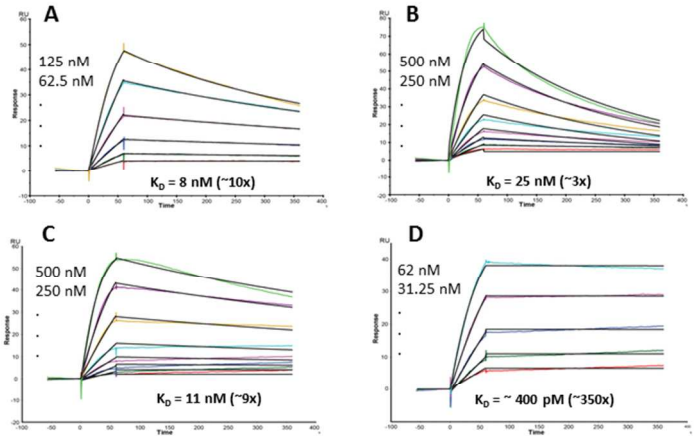


254x190mm (96 x 96 DPI)

Figure 7

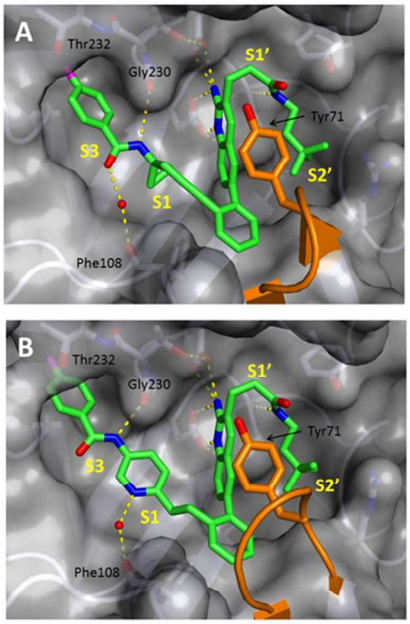


254x190mm (96 x 96 DPI)